

## Chapter 2

# Loads and Material Properties for Nuclear Facilities – A General Survey

### 2.1 Introduction

The probable failure assessment of structures for nuclear power facilities has bearings on the choice and postulation of the loads and load combinations, since the exact magnitude of the loads encountered in nuclear power plant design cannot be easily predicted. The loads are normally treated as random variables. These loads are generally defined in terms of probability of strength in different components/elements of structures for a nuclear facility. Together with the strength characteristics of elements, it would be possible to determine the probability of the structure being able to perform the functions for which it has been designed. For obtaining reliable results a proper accounting of uncertainties practically at every stage of stress determination is necessary. The stress determination is the end product of

- (a) the analysis and prediction of postulated even loads;
- (b) the probability distribution of different variables involved causing the loads to occur. One form is the statistical sampling technique. The data and probability distribution will lead to the load to be considered.

In addition to the two load levels considered in conventional design, nuclear facilities are typically designed for third load level, termed the extreme load. Extreme loads include such natural phenomena as the maximum earthquake potential for a site considering regional and local geology, seismology, local foundation conditions, tornado wind and associated air-borne missile loads. It also includes postulated design basis accident loads consisting of high-energy system rupture that results in pipe break reaction and impingement loads, pipe whip and associated accident-generated missiles and pressurisation of building components, flooding and high thermal transients.

In the USA structures for nuclear facilities are designed for service load conditions. Three methods are recommended such as working stress design (WSD), factor load design (FLD) and factor load reduction design (FLRD). In Europe the limit state design (LSD) is generally recommended using partial safety factors for materials and loads or actions. Where service load design parameters and material strength data for nuclear facilities are not given or

**Table 2.1** Service load parameters

Loads or stresses	Design load or range of actions	Notation
Dead load		$D$
Reinforced/prestressed Concrete	$6.7 - 7.5 \text{ kN/m}^2$	dead load
Structural steel	$24 \text{ kN/m}$	
Structural aluminium		
Structural wood		
I. S—snow load	Specified: ANSI A58.1 100-year interval or BS6399 Part 2 (see text table in this chapter)	L,LL Live or imposed or action
II. Construction	$1.73 \text{ kN/m}^2$	Co
III. Buoyancy	$0.91 \text{ kN/m}^2$	$B$
IV. Earth pressure (lateral)		$E_p$
(a) Active	Foundation below grade $3.14 - 18.84 \text{ kN/m}^2/\text{m}$ $3.14 - 70.65 \text{ kN/m}^2/\text{m}$ $6.28 - 23.55 \text{ kN/m}^2/\text{m}$	
(b) Passive		
(c) At rest		
V. Piping equipment reaction	Depends on the piping analysis $\rightarrow$ variable	$R_t$
VI. Hatch for containment equipment	$67 \text{ kN/m}^2$	$H_e$
(a) Uniform load assumed	$2000 \text{ kN}$	$H_p$
(b) Concentrated load moving type		
Note: Not concurrent with uniform lived load		
(c) Personnel hatch uniform load moving type	$67 \text{ kN/m}^2$ $44.5 \text{ kN}$	
VII. Linear for concrete containment		
(a) Concentrated load	$6.67 \text{ kN}$	
(b) Line load	$2.2 \text{ kN/m}$	
(c) Uniform load	$25 \text{ kN/m}^2$	
VIII. Uniform floor load		
(a) Reactor building operating deck	$1675 \text{ kN/m}^2$	
(b) Stairs, passage and escalator/moving walks	$67 \text{ kN/m}^2$ (uniform) Plus concentrated from manufacturer B	
IX. Wind load	$F_w = q_{\text{ref}} \cdot c_e(z_e) \cdot c_d \cdot c_{fi}(A_{\text{ref}})$ where $z_e$ height above ground $q_{\text{ref}}$ mean wind velocity pressure $c_f$ derived force coefficient $c_e$ exposure coefficient; $c_d$ dynamic factor	$W$ or $F_w$ $P$

Table 2.1 (continued)

Loads or stresses	Design load or range of actions	Notation
	$c_{fi}$ force coefficient	
	$A_{ref}$ reference area of $c_f$	
	$v_{ref} = c_{DIR} \cdot c_{TEM} \cdot c_{ALT} \cdot v_{refo}$	
	$v_{refo}$ basic value of reference wind velocity	
	$c_{DIR}$ directional factor taken generally as 1.0	
	$c_{TEM}$ seasonal factor taken generally as 1.0	
	$c_{ALT}$ altitude factor taken to be 1.0 unless specified	
(b) Based on BS6399	$q_{ref}$ = wind mean velocity pressure $X_{v_{ref}} = Fw$	
	$V_s$ = site velocity = $V_o S_a S_d S_s S_p$	
	$V_b$ = basic wind speed $\rightarrow v_{refo}$	
	$S_a$ = altitude factor $\rightarrow c_{ALT}$	
	$S_d$ = Direction factor $\rightarrow c_{DIR} = 1$	
	$S_s$ = seasonal factor $\rightarrow c_{TEM} = 1$	
	$S_p$ = probability factor = 1	
	$q$ = wind dynamic pressure = $k V_s^2$	
	where $k = 0.613$	
	$V_e = V_s \times V_p$ – terrain factor	
	Example for $V_b = 45$ m/s; $s_1 = 1$ ; $s_2 = 0.83$	
	<i>Solution based on BS 6399</i>	
	$V_b = V_o S_a S_d S_s S_p$ ;	
	$V_b$ = basic wind speed = 23.5 m/s	
	$S_a = 1 + 0.001 \times 100 = 1.1$	
	$S_p = 1.0$	
	$S_s = 0.62$	
	$S_p = 1.0$	
	$V_s = 16.03$ m/s	
	$V_e = S V_s S_b$	
	$S_b = S_c T_c [1 + (g_t S_t T_y) + S_h]$	
	$= 1.08(0.863)[1 + (2.52 \times 1.71 \times 1.38) + 0]$	
	$= 1.486$	
	$V_e = 16.03 \times 1.486 = 23.82$ m/s	
	$q$ = dynamic pressure	
	$= 0.613(23.83)^2 = 348$ N/m <sup>2</sup>	
$P$ = net wind load on the surface	where	
$P = p A_{ref}$	$S_c$ = fetch factor	
$P$ = net pressure across the surface	$S_h$ = topography factor	
(c) American codes	$S_t$ = turbulence factor	
	$g_f$ = gust factor	
	$T_y$ = Turbulant adjust factor	
	$T_c$ = fetch factor for adjustment	$P_{cont.}$
	ANSI A58.1 for exposure C Fig. 2 of the code	To
	Load based on 100-year recurrence wind, speed with gust factor and wind profile distribution	
X. Containments Internal Pressure	$p \nlessgtr 345$ kN/m <sup>2</sup> for PWR	

**Table 2.1** (continued)

Loads or stresses	Design load or range of actions	Notation
<b>XI. Operating thermal load</b>		
(a) Thermal gradients through the wall of containment	−11.2 (outside) + 6.672°C (inside) +5.5 (outside) + 6.672°C (inside)	
(b) Range of ambient temperatures at placement of concrete in containment	22.24 < <i>t</i> < 50°C	
(c) Thermal gradient through reactor coolant compartment walls	±16.7°C gradient	<i>V</i>
(d) Range of ambient temperatures at placement of concrete	55.6°C < <i>t</i> < 6.7°C	
(e) Thermal gradients through spent fuel pit walls	6.67°C max.mean temperature 4.5°C min.mean temperature −11.2 (outside) + 100°C (inside)	
<b>XII. Resulting from the internal drop in containment (load)</b>	0.13 kN/m <sup>2</sup>	
<b>XIII. Internal pressure for advanced cooled reactor vessels</b>	≥ 6900 kN/m <sup>2</sup>	
<b>XIV. Combination of Actions and Load Factors at the ultimate state</b>	<i>G<sub>k</sub></i> <i>Q<sub>k</sub></i> <i>W</i> or <i>W<sub>k</sub></i> 1.0    0    1.5 1.0    0    1.5 1.0    0    1.5	
(a) Permanent + variable	1.4    1.5	
(b) Permanent + wind + variable	1.4    0    1.5	
(c) Permanent + variable		
(d) Permanent + wind		
<b>XV. Prestressed concrete reactor pressure vessel</b>	Loadings	<i>P<sub>o</sub></i> <i>P'</i>
Load combinations for elastic/work analysis	<i>Case 1</i> Prestress and ambient temperature <i>Case 2</i> Prestress 1.15 × design pressure + ambient temperature <i>Case 3*</i> Prestress + design pressure + temperature <i>Case 4*</i> Overload (prestress + increasing pressure + temperature)	
	* Short- and long-term conditions apply	
$P' = P_0(\text{transfer force}) - \alpha$ $\infty$ = Losses in tendons $P_o$ = (transfer force) $F_{\text{rdu}} = P$	$= \bar{\alpha} f_{\text{ck}} \left[ \frac{A_{\text{cl}}}{A_{\text{co}}} \right]^{0.5} \leq 2f_{\text{ck}}$ $\bar{\alpha}$ = depending upon adopted system range 0.67–0.85 $A_{\text{cl}}$ = loaded area of the anchorage plate $A_{\text{co}}$ = Anchorage area of the concrete block or block of material	

**Table 2.2** Concrete stresses based on American and European codes

Stresses	Design stresses under range of actions	Notation
1. Concrete stresses based on ACI 359		$f'_c, f_{ck}$ Cylindrical Strength
<i>Containment—primary</i>		
(a) Membrane	$0.35f'_c$	
(b) Membrane plus bending	$0.45f'_c$	
<i>containment—secondary</i>		
(a) Membrane	$0.45f'_c$	
(b) Membrane plus bending	$0.60f'_c$	
concrete (after losses)		
<i>Containments—primary</i>		
(a) Membrane		
(b) Membrane plus bending		
<i>Containment—secondary</i>	$0.30f'_c$ $0.45f'_c$	
2. Euro code 2		
<i>Concrete material properties</i>		
$f_{ck}$ = cylindrical strength	25 – 60 N/mm <sup>2</sup> 90 $\geq$ N/mm <sup>2</sup>	
$f_{ck}, \sigma_u$ = minimum cube	–41.34 kN/mm <sup>2</sup>	
Strength of concrete at 28 days		
$f_y, \sigma_y$ = yield strength	–0.66 $\sigma_{cu}$	
$\sigma_t$ = tensile strength	+0.1 $\sigma_{cu}$	
$E$ = elastic modulus	+41.4 kN/mm <sup>2</sup>	
$E_p$ = plastic modulus	+0.476 $E$	
$\epsilon_{cu}$ = ultimate strains	0.0035	
$\nu$ = Poisson ratio	0.18	
$\alpha_T$ = coefficient of linear thermal expansion	8.0 $\mu$ M/m°C	
$K$ = thermal conductivity	1.75 W/m°C	
$a'$ = coefficient of aggregates	0.65, 0.68, 0.87, 0.87	
$\epsilon_{ct}$ = shrinkage strain	$200 \times 10^{-6}$	
<i>Conventional steel</i>		
$\bar{\gamma} = \sigma_y$ = yield strength	4516 MN/mm <sup>2</sup> (50 $\omega$ ) or $T50$	
$E$ = elastic modulus	4400 (25 $\omega$ ) or $T25$	
$E_p$ = plastic modulus	200 kN/mm <sup>2</sup>	
$\alpha_T$ = coefficient of linear concrete thermal expansion	0.1 $E = 20$ kN/mm <sup>2</sup>	
$f_{yk}$ = characteristic strength	500 N/mm <sup>2</sup>	
<i>Liner</i>	12 mm + 10%	
$t_s$ = thickness	19 mm + 5%	
	Up to 40 mm max to 400 mm up to	
$\bar{Y} = \sigma_y$ = yield strength	25 mm up to 25 m	
$\alpha_t$ = coefficient of linear thermal expansion	$3.4 \times 10^5$ kN/mm <sup>2</sup> 10 $\mu$ M/m°C	
$K$ = thermal conductivity	41.6 W/m°C	
<i>Prestress</i>	Reference is made to the manufacturer's catalogues for various systems	
$f_{mas}$ (at service)	0.6 – 0.75 $f_{ck}$	
$f_{mas}$ (at service)	0.6 $f_{max} = P_o$ transfer force : see catalogues for systems for accurate assessment	

**Table 2.3** Structural steel

Service load parameters and stresses		
Loads or stresses	Design load or range of actions	Notation
1. Structural steel based on EC-3		
(a) Conventional steel design, load combinations		
Dead load	$1.46G_k$ or $Y_f F_k$	$D$
Dead load + restraining overturning	$1.0G_k$	
Dead + imposed load	$1.4G_k + 1.6Q_k$	
Dead + imposed + wind	$1.2(G_k + Q_k + W_k)$	
$E'_c$ recent version		
$F_d$ design action		
2. Structural steel Euro codes-3 (EC-3)	$\gamma_G = 1.35 : \gamma_Q = 1.5$	
(a) Grade shapes S275		Grade S
	$F_y$ = design strength	
	$F_e 430 \leq 16$	
	$\leq 40$	
S355	$F_e 510 \leq 16$	
	$\leq 40$	
(b) Quenched tempered plates	$f_y = 690 \text{ N/mm}^2$	
(c) Alloy bars – tension members	$f_y = 1030 \text{ N/mm}^2$	
(d) High-carbon hard-drawn wires for cables	$f_y = 1700 \text{ N/mm}^2$	
3. Load and resistance factor design (LRFD)	$R_u \leq \phi R_n$ ;	$\phi$
(a) The design strength must equal or exceed the required strength $R_u$	$R_n$ = safe working load $\times$ safety factor	
(b) Required strength and load combination for LRFD based on ASCE-7 Section 2.3	$R_n$ = normal strength determined LRFD load combinations	
	$\phi$ = Resistance factor given by the Specification for a particular limit state	
	0.5	
	1.4D	
	$1.2D + 1.6L + 0.5(L_r \text{ or } S \text{ or } R)$	
	$1.2D + 1.6(L_r \text{ or } S \text{ or } R) + (0.5L \text{ or } 0.8W)$	
	$1.2D + 1.6W + 0.5L + 0.5(L_r \text{ or } S \text{ or } R)$	
	$1.2D \pm 1.0E + 0.5L + 0.2S$	
	$0.9D \pm (1.6W \text{ or } 1.0E)$	
	$D$ = dead load	
	$L$ = live load due to occupancy	
	$L_r$ = roof live load	
	$S$ = snow load	
	$R$ = nominal load due to initial rainwater or ice	
	$W$ = wind load	
	$E$ = earthquake load	

**Table 2.3** (continued)

Service load parameters and stresses		
Loads or stresses	Design load or range of actions	Notation
	LRFD	$\Delta$
	$M_r = B_1 M_m + B_2 M_u = B_2 M_u$ $P_r = P_{nt} + B_2 P_{it} = B_2 P_u$ $B_1 \leq 1.05 \nless B_2$	
(c) Simplified determination of required strength based on LRFD. Based on effective length method where P- $\delta$ factor is small	$B_2 > 1.5$ simplified method is not valid $\frac{\Delta_{2nd}}{\Delta_{1st}} \leq 1.5$ storey gravity load = minimum 2% $K = 1$ for braced frame $K$ value to be determined for moment frames using sideway buckling analysis	
(d) Stability design	or $P_r \leq 0.5 P_y$ ; $\alpha = 1.0$ for LRFD $P_r$ = required axial compressive strength $P_y$ = member yield strength = $AF_y$	
(e) The required compressive strength contributing to stability (lateral) by flexural stiffness	$P_n = 2tb_{\text{eff}}.F_u$ $\theta_r = 0.75$ for LRFD $P_n = 0.6F_u A_{sf}$ ; $A_{sf} = 2t(a + d/z)$ $a$ = shorter distance from the edge in mm	
(f) Pin connected members	$d$ = pin diameter in mm	
i. Tensile strength	$t$ = plate thickness in mm	
	$b_{\text{eff}} = (2t + 16 \text{ mm})$	
ii. Shear rupture	<i>Note:</i> For complete design specifications, a reference is made to steel construction manual (AISCE) 13th edition Dec 2005 ISBN 1-56424-055x or forward editions	

**Table 2.4** Aluminium

Service load parameters and stresses		
Aluminium structures		Notation
Aluminium structures		
Characteristic values based on Euro code-9		
$f_u$ = ultimate strength	$L$ = longitudinal = $310 \frac{N}{\text{mm}^2}$ Temper T6	
$f_o$ = 0.2% proof strength	$T$ = transfer = $260 \text{ N/mm}^2$	
	$A$ = minimum elongation = 6%; Buckling class A	
(a) Alloy EN-AW 6082 100 mm thickness	$E = 74,000 \text{ N/mm}^2$ $G = 27,000 \text{ N/mm}^2$ $\nu$ = Poisson's ratio = 0.3 $\alpha$ = coefficient = $23 \times 10^{-6}$ per $^\circ\text{C}$ of linear expansion $P$ = unit mass = $2700 \text{ kg/m}^2$	
(b) 6061	$T6/T651$ thickness $< 12.5$ $f_o = 110 \text{ N/mm}^2$ $f_u = 205 \text{ N/mm}^2$ $A_{so} = 12$	
(c) Bolts for 6082 T6 aluminium alloy	$\text{dia} \leq 6$ $f_o = 250 \text{ N/mm}^2$ $f_u = 320 \text{ N/mm}^2$	

**Table 2.5** Structural composites

Service load parameters and stresses		
Loads or stresses	Design load or range of actions	Notation
<i>Structural composites based on EC-4</i>		
(a) Design parameters $b_e$		
$b_e$ = effective breadth $L_z$ = distance between points of zero moment	$L_z/8 \nlessgtr$ half the distance of adjacent beam	$b_e$
Concrete slab stress	$0.45f_{ck}$	
Steel stress	$0.95f_y$	
$p_v$ = shear capacity		$P_v$
Moment		$M$
$M_{api.RD} > M_{cd}$		
Moment resistance of the steel beam	$W_{pl}f_d$	
$R_c$ = compressible resistance of slab	$0.85f_{ck}/\gamma_c \times b_{eff} \times b_c = 0.45f_{ck} b_{eff} b_c$	$R_c$
$f_{ck}$ = concrete cylindrical strength	$0.85f_{cu}$ or $0.8f_{k(cu)}$ $\gamma_f$ = partial safety factor = 1.5	$f_{ck}$
$R_s$ = compressive resistance of steel section	$f_d A_a$	$M_{pl,Rd}$
$M_{pl,Rd}$ = moment or resistance of composite beam	$R_s [\frac{h}{2} + h_c + h_p - R_s^{h_c}/2R_c]$	
$V_{pl,Rd}$ = shear resistance	$f_y A_v / (r_a \sqrt{3})$ $0.5V_{pl,RD} > V_s d$	
<i>Shear connector</i>		
Failure of concrete		
$P_{Rd}$	$0.29\alpha d^2 \sqrt{Cf_{ck}E_c\gamma_r}$ or $R_d = \frac{0.8f_u\pi d^2}{4\gamma_v}$ shear failure of the steel at its weld	

available, the data given in this chapter shall be adopted by individual clients or their consultants. Tables 2.1, 2.2, 2.3, 2.4 and 2.5 give data on service load parameter and relevant acceptable stresses for the design of conventional structures for nuclear facilities, within the USA. In addition the Euro codes are mentioned for the design of conventional structures called ancillary or auxiliary structures associated with nuclear facilities. Loads (actions) and stresses are tabulated from the US and the European codes. For detailed design a reference is made to the relevant codes where necessary.



## **2.2 Loads**

### **2.2.1 Service Loads**

Service load conditions are those loadings encountered during construction and in the normal operation of nuclear power facilities. A suggested summary of the list of loads is given below.

#### **2.2.1.1 Dead Load ( $D$ )**

Dead load is vertical load due to the weight of all permanent structural and non-structural components of a building, such as walls, floors, roofs and fixed service equipment as specified by the relevant codes and standards such as BS6399.

#### **2.2.1.2 Operating Live Load ( $L$ )**

Live load is the load superimposed by the used and occupancy of the building not including the wind load, earthquake load and impact load as specified by the relevant codes and standards.

#### **2.2.1.3 Uniformly Distributed Loads ( $LL$ )**

The live load is to be assumed in the design of building and other structures shall be the largest loads that can be expected to be produced by the intended use or occupancy, but in no case shall be less than the minimum uniformly distributed unit loads specified by the relevant codes and standards such as BS6399-1 to 3 or EC2, EC3.

#### **2.2.1.4 Concentrated Loads ( $L_c$ )**

Floors shall be designed to support safely a concentrated load simultaneously with the floor live loads. In European codes it is termed as knife edge loads.

#### **2.2.1.5 Railroad Support ( $C_E$ )**

For design purpose Cooper's E-72 loading should be used unless otherwise specified by intended use, such as support spent fuel cask handling car or other heavy equipment.

#### **2.2.1.6 Truck Support ( $H_{20}$ )**

For design purposes, AASHO H-20-S16 loading should be used unless otherwise specified by intended use. The equivalent European track load can also be adopted instead.

### 2.2.1.7 Ordinary Impact Loads (*I*)

#### Machinery

The weight of machinery and moving loads should be increased to allow for impact. Some suggested values are 100% for elevator machinery; 20% for light machinery, shaft or motor driven; 50% for reciprocating machinery or power-driven units. All percentages should be increased or decreased as required by the design specification or manufacturer's recommendation.

#### Craneways

It is suggested that all craneways have their design loads increased for impact as follows: A vertical force equal to 25% of the maximum wheel load; a lateral force equal to 20% of the weight of trolley and lifter load only, applied one-half at the top of each rail; and longitudinal force of 10% at the maximum wheel loads of the crane applied at the top of rail. All percentages shall be increased or decreased if so recommended by the manufacturer or if otherwise specified by governing codes.

### 2.2.1.8 Construction Loads

Consideration shall be given to temporary large, heavy loads based on the 'Building Codes Requirements for Minimum Design Load in Building and Other Structures' (ANSI A58.1-1972)[1]. These provisions specifically exclude consideration of tornadoes. For extreme loads due to tornadoes, Section 3.3.2 should be referred to. Account should be taken of hurricane winds by comparison with the provisions of Section 3.3.3 for hurricane-susceptible sites. While using European codes a reference is made to BS6399, part 2 and Eurocode ENV1991-2-4 for wind loading. Table 2.1 part IX gives a brief relevant equation for the determination of loads caused by the wind.

### 2.2.1.9 Snow Loads (*S*)

Basic snow load requirements as a function of geographical area can also be found in ANSI Standard A58.1972. Table 2.1 gives a brief based on European code BS 6399-2-4.

#### Soil and Hydrostatic Pressure ( $E_p$ ) and Buoyancy ( $B$ )

In designing nuclear facilities which are partly or wholly below grade, provision shall be made for the lateral pressure of adjacent soil, namely active pressure and at-rest pressure. The effect of dynamic pressure due to earthquake also should be given consideration. Due allowance shall be made for possible surcharge from fixed or moving loads. When a portion or the whole of the adjacent soil is below a free-water surface, computations shall be based on the weight of the soil diminished by buoyancy plus hydrostatic pressure. In the design of slabs

below grade, the upward pressure of water, if any, shall be taken as the full hydrostatic pressure applied over the entire area. The hydrostatic head shall be measured from the underside of the slab. These are recommended also by the Nuclear Regulatory Commission (NRC) and ASCE of the USA.

### Piping Equipment Reaction Load ( $R_o$ )

Piping system is attached directly to building structures through hangers, struts, restraints, anchors and snubbers. Hangers and struts are unidirectional, transmitting loads in one direction only. Hangers transmit only vertical loads. Restraints will transmit loads in any one or more of the coordinate directions. Anchors are capable of transmitting loads and moments in all three coordinate directions. Snubbers are unidirectional and transmit dynamic loads only.

Equipment loads include dead weight, restrained thermal expansion and dynamic effect such as pressure transients, changes in momentum, water and steam hammer in the equipment and earthquake. They also may include the effect of the restraint of attached piping. The effect of such phenomena must be considered in the design check.

### Operating Pressure and Temperature ( $P_o$ , $T_o$ )

In many cases compartments or sub-compartments within a structure which house highly radioactive pipes or equipment are maintained at lower pressure than the outside of the compartment in order to prevent out-leakage. Even though the differential pressure is not considerable, the magnitude should be determined and its effect evaluated particularly for steel structures which are more likely to experience external pressure buckling modes of failure.

### 2.2.2 *Operating Basis Earthquake ( $E_o$ )*

The respective nuclear organisation and regulatory commissions have criteria for the seismic design of nuclear power plants. The Operation Basis Earthquake (OBE) does consider the effect on a plant site during the operational life of the plant. Both local geology and seismology are related to specific characteristics of local subsurface materials.

Earthquakes can cause local soil failure, surface ruptures and structural damage of nuclear power plants. The most significant earthquake effects on plants or their structural components result from the seismic waves which propagate outwards in all directions from the earthquake focus. These different types of waves can cause significant ground movements up to several hundred miles from the source. The movements depend upon the intensity, sequence, duration and the frequency content of the earthquake-induced

ground motions. For design purposes ground motion is described by the history of hypothesised ground acceleration and is commonly expressed in terms of response spectrum derived from that history. When records are unavailable or insufficient, smoothed response spectra are devised for design purposes to characterise the ground motion. In principal, the designers describe the ground motions in terms of two perpendicular horizontal components and a vertical component for the entire base of the nuclear power plants. A 3D analysis is essential using hybrid finite element non-linear method.

When the history of ground shaking at a particular site or the response spectrum derived from this history is known, plants' theoretical response can be calculated by various methods; these are described later.

The minimum acceptable acceleration for the OBE will be taken at least one-half of the Safe Shutdown Earthquake (SSE) acceleration. Sometimes  $OBE < SSE$  have been permitted in some cases where SSE return period is such duration as not to be reasonably expected during the life of the nuclear power plant. If the vibratory ground acceleration of the site is equal to or greater than OBE acceleration, the US Federal Regulation makes it mandatory to shut the nuclear power plant for inspection.

### 2.2.2.1 Response Spectra

The main cause of the structural damage during earthquake is its response to ground motion which is in fact input to the base of the structure. To evaluate the behaviour of the plant under this type of loading condition knowledge of structural dynamics is required. The static analysis and design can now be changed to separate time-dependent analysis and design. The loading and all aspects of response vary with time which result in an infinite number of possible solutions at each instant during the time interval. For a design engineer the maximum values of the plant response are needed for the structural design.

The response may be deflection, shear, equivalent acceleration, etc: the response curves are generally similar with majority variations occurring in the vertical coordinates. The variation occurs with magnitude of the earthquake and the location of the recording instruments. Accelerations derived from actual earthquakes are surprisingly high as compared with the force used in designs and the main reason is the effect of different degrees of damping.

The recorded earthquake ground accelerations have no doubt similar properties to those of non-stationary random functions but owing to a lack of statistical properties related to such motions artificially generated accelerograms are used which are flexible for any duration.

The following three major aspects must be considered:

- (a) Location of vibratory ground motion for OBE
- (b) Direction of motion for OBE
- (c) Vertical Acceleration associated with OBE

This book covers all aspects in detail when earthquake analysis of nuclear plant is considered. The reader is advised to examine the author's book on *Earthquake-Assistant Buildings* published by Springer-Verlag, Germany (2010) particularly using analyses and loadings with and without seismic devices.

### **2.2.3 Extreme or Severe Loads**

These loads include extreme environmental conditions, such as tornadoes and the safe shutdown earthquake postulated to occur during the life of the facility. Also included are effects resulting from a postulated rupture of a high-energy system during normal operation, startup or shutdown of the plant or other postulated design basis accident.

#### **2.2.3.1 Safe Shutdown Earthquake ( $E^1$ )**

The Nuclear Regulatory Commission's Federal Regulation 10 CFR 100 Appendix A, entitled 'Seismic and Geology Siting Criteria for Nuclear Power Plants' sets forth principal seismic and geological considerations which shall be used by the Commission in its evaluation of the suitability of proposed sites for nuclear power plants. Contained within this Appendix are definitions and procedures which are to be used as guidelines in establishing the various seismic input motion and potential faulting hazard for nuclear power plants, in the USA. Specifically, the safe shutdown earthquake (SSE) is defined as that earthquake which produces the vibratory ground motion for which structures, systems and components are important for safety of the structures or systems.

#### **Required Investigations**

Paragraph IV entitled 'Required Investigations.' in Appendix A of 10 CFR 100 sets forth the required geologic and seismic investigations that should be carried out to establish vibratory ground motion requirements and surface faulting. Sub-paragraph A entitled 'Required Investigation for vibratory Ground Motion' sets forth the specific investigations that should be carried out to establish the ground motion input associated with the SSE. Briefly, the items that should be considered to establish the ground motion input associated with SSE are as follows:

1. geologic conditions at the site;
2. tectonic structure determination;
3. identification of effects of prior earthquakes;
4. determination of static and dynamic characteristics of underlying materials;
5. historical listings of all earthquakes which may have affected the site;
6. correlation of epicentre;
7. determination of fault locations;
8. characteristics of faults in the vicinity.

*Locations of Vibratory Ground Motion for SSE* should be considered to be acting at the ground surface in the free field. The maximum acceleration of the vibratory ground motion for the SSE should be considered on the basis of evaluating the result of the investigation as stated above required investigation. The guideline shall be on this maximum acceleration as the largest possible acceleration at the site due to a postulated fault activity.

The direction of motion for SSE shall generally be assumed as resultant motion to correspond with one of the principal horizontal directions of the structure for the facility being analysed.

The vertical motion associated with SSE can be established on the basis of the information developed from the above-mentioned investigation. The value should not be less than  $2/3$  of the maximum horizontal ground acceleration of the SSE. The frequency strength is between 3.5 and 33 Hz. The vertical acceleration shall be equal in intensity to the horizontal component.

### 2.2.3.2 Tornado Loads ( $W_t$ )

Structures for the nuclear facility shall be designed to resist the maximum tornado load for a given plant site. The basis of the design shall be such that the safety class equipment remains functional; even a safe shutdown of the facility is accomplished in totality without endangering the plant. The AEC Regulatory Guide 1.76 recommends the design basis tornado.

The effects of a tornado that are manifested in structural damage are generated from three separate phenomena: wind, differential atmospheric pressure and missiles. These effects interact with structures and cause damage through three principal mechanisms:

1. pressure forces created by drag and lift as air flows around and over structure;
2. pressure forces created by relatively rapid changes in atmospheric pressure resulting in differential pressure between the interior and exterior of the building;
3. penetration, spalling and impact forces created by missiles.

*Tornado missiles ( $Y_m$ ):* Tornado-generated missiles carry objects which are accelerated by the forces induced by the extreme wind speeds of the tornado. The parameters specified in the design basis tornado are translated into pressures and forces acting on the structures and its components. The important case is the real analysis that would be necessary to perform on the structure. The analysis is known as tornado structure interaction. In this analysis the load evaluated using a specific path width of the tornado field that experiences wind velocities  $\geq 75$  mph (120 km/h) is generally considered.

### 2.2.3.3 Hurricane Loads

A hurricane by definition is a cyclone storm having rotational wind velocities in excess of 70 mph (119 km/h). The dynamic strength of a hurricane builds up over water, but as it comes inland boundary layer drag forces cause a tremendous dissipation of the kinetic energy of the storm and the wind.

As regards wind distribution which is one aspect of hurricane loads, the maximum wind velocities generally occur to the right of the eye of the hurricane looking along the direction of its path. This is due to vectorial addition of the translational and rotational components of the wind. The following data can be adopted in the absence of specific data not available for the site under consideration:

1.  $\alpha$  = Inclination of the direction of the wind =  $20-30^\circ$  (towards the centre of the hurricane)
2. Wind gust > the sustained wind by 30–50%
3. Hurricane diameter: 15 miles (24 km) to 100 miles (160 km)
4. Gale force wind: 40 mph (64 km/h occurring within 30 miles (560 km) to 400 miles (640 km)

Where sea swell surge and flooding occur, specific calculations would be required to algebraically evaluate the additional load occurring when considered along with other loads.

### 2.2.3.4 Tsunami Loads

Tsunami are long ocean water waves generated by mechanisms such as earthquakes or underwater explosions, which impinge on coastal areas. With regard to earthquakes tsunami appeared to be primarily associated with those tectonic movements having substantial vertical components of motion (dip-slip). The design of nuclear facilities to resist the effects of tsunami must be undertaken for all nuclear site adjacent to coastal areas, especially those bordering the Pacific Ocean. The basic criteria for tsunami are set forth in the NRC's Standard Format and the Contents of Safety Analysis Reports for Nuclear Power Plant. These silent feature must be known such as the

- (i) Location relevant to the site
- (ii) Magnitude
- (iii) Tsunami wave height
- (iv) Influence of harbour/break water and hydrography
- (v) Records of the region with valuable statistics

The direct dynamic force of the moving tsunami wave impinging against structures of power facilities shall be algebraically added to the force produced due to the impact of the floating debris and water-borne missiles.

### 2.2.3.5 Missile Load ( $Y_m$ )

In nuclear facility design, safety class structures shall be protected against loss of functions due to postulated plant generated and extreme environmental missiles depending on aircraft crash should be considered.

The effect of missile impact on a target on the material and geometric properties of the impacting bodies. The phenomenon can be described in general as the formation of an impulse measured by the momentum exchange between the two bodies during the impact. Table 2.6 gives data on tornado and wind-generated missiles.

**Table 2.6** Tornado and wind-generated missiles and their characteristics: wood, steel and concrete building components

Service load parameter and stresses					
Missile type	Geometry				
	Diameter (mm)	Length (m)	Impact area (m <sup>2</sup> )	Velocity (m/s)	Weight (kg)
Wooden plank	—	3.67	0.03	41.5	56.7
Wooden pole	200	3.67	0.03	5.73	94.8
Circular hollow sections in steel (average)	168.3	4	0.000026	70.2	60
Sign boards (average)	—	—	6.0	57	56
Steel I-beam light sections (average)	—	4	0.000032	40.5	100
Steel members channel sections (average)	—	3	0.000013	50.5	30
Steel members L-sections (average)	—	3	0.000015	45.5	36
Steel rafters T-sections (average)	—	3	0.000018	45.5	42
Steel rod	25	0.92	0.00049	75.6	3.63
Concrete lintels	—	3	0.025	60.5	1.8
Concrete sleepers	—	2.7	0.0031	75	0.2
Precast concrete beams or piles at delivery stage	—	9	0.09	60.5	19.44
Precast concrete wall panels	—	5	11.5	2.5	1380
Prestressed concrete pipes	400	—	—	—	1.1
	500	—	—	—	1.375
	600	—	—	—	1.65
	700	—	—	—	1.92
	800	—	—	—	2.2
	900	—	—	—	2.474
	1676	6	0.032	—	4.608
Prestressed concrete poles	—	17	0.0019	30.5	65.7
	—	12	0.0008	50.1	14.46
	—	9	0.000025	65.2	9.65



Missiles are usually classified by source as plant (accident)-generated missile and extreme environmental missiles. Typical plant-generated missiles include valve stems, valve bonnets, (caused by rupture of high-energy systems) and turbine discs and other rotating masses (caused by rupture of rotating parts). Extreme environmental missiles which are of major concern include tornado-generated missile and aircraft.

Table 2.7 gives a list of plant-generated missiles and their characteristics. They depend on their region, ranges of size, weight and impact velocity.

Tables 2.8, 2.9, 2.10, 2.11, 2.12, 2.13, 2.14 and 2.15 give various aircraft parameters and their characteristics and impact parameters.

**Table 2.7** Plant-generated missile and their characteristics

Service load parameters and stresses			
Missile type	Weight (kg)	Impact area (cm <sup>2</sup> )	Velocity (m/s)
Control rod mechanism or fuel	53	15.5	91.5
Disc 90° sector	1288	495	125
Disc 120° sector	1600	6573	156
<i>Hexagon head bolts</i>			
1.4 cm dia	0.20	1.54	250
2.0 cm dia	0.30	2.30	230
2.4 cm dia	0.37	2.84	189
3.3 cm dia	0.42	3.22	150
6.8 cm dia	0.97	7.44	100
<i>Turbine rotor fragments</i>			
<i>High trajectory</i>			
Heavy	3649	5805	198
Moderate	1825	3638	235
Light	89	420	300
<i>Low trajectory</i>			
Heavy	3649	5805	128
Moderate	1825	3638	162
Light	89	420	244
<i>Valve bonnets</i>			
Heavy	445	851	79
Moderate	178	181	43
Light	33	129	37
<i>Valve stems</i>			
Heavy	23	25	37.5
Moderate	14	9.7	20
<i>Others</i>			
30 cm pipe	33.7	260	68
12 cm hard steel disc	1.6	113	140
Steel washer	0.0005	3	250
Winfirth test missile	15.6	176	240

**Table 2.8** Civilian sircraft

Service load parameters and stresses	
Data on civilian and military aircraft	
Civilian aircraft normally in service includes Concorde, Airbus, Boeing, Antonov, Ilyushin and Tupolov	
$S$ = span; $L$ = length; $H$ = height; $A_w$ = wing area; $P_L$ = payload $V$ = speed; $W_a$ = weight at take-off or loading	
Basic parameters of Concorde	
Power Plant	
$4 \times 38,050$ lb (169 kN)	
Rolls-Royce/Sneema Olympus	
593 Mk60 two-spool turbojet	
$S$ (m)	25.61
$L$ (m)	62.1
$H$ (m)	12.19
$A_w$ (m <sup>2</sup> )	358
$P_L$ (kg)	11,340
$V$ (km/h)	2150
$w_a$ (kg)	186,800

Tables 2.16, 2.17, 2.18, 2.19, 2.20, 2.21, 2.22 and 2.23 dictate again various military missiles with their characteristics and impact parameters.

For details and in-depth study references are made to the following authors:

- (a) *Impact Explosion Analysis and Design*, Blackwell, 1993.
- (b) *Manual of Numerical Methods in Concrete*, Thomas Tefford.
- (c) *Shock, Impact & Explosion*, Springer, 2008.

### 2.2.3.6 Design Basis Accident Load

In addition to accident-generated missile loads there are several loading phenomena generated as the result of a design basis accident which normally includes all postulated high-energy system ruptures. Included in this category are all accident-induced pressure and temperatures, as well as high-energy fluid jet impingement and rupture reaction loads. The criteria for defining design basis high-energy system ruptures are found in the NRC Standard Review Plan.

#### Accident Pressure ( $P_a$ ) and Temperature ( $T_a$ )

These pressures and temperatures are typically developed as a result of the blowdown of a high-energy system into a confined space. They typically include the containment design pressure and temperature as well as differential pressure and temperature across interior partitions or structures which house ruptured high-energy systems.

Table 2.9 (a) Data on the Airbus family and (b) data for Antonov aircraft

Type	Power plant	$S$ (m)	$L$ (m)	$H$ (m)	$A_w$ (m <sup>2</sup> )	$P_L$ (kg)	$V$ (km/h)	$W_a$ (kg)
(a) Data for Airbus family								
A300B2-100	2×51,000 lb (227 kN) GE CF6-50C turbofans	44.84	53.75	16.53	260	14,900	869	34,585
A300B2-200	2×51,000 lb (227 kN) GE CF6-50C turbofans	44.84	53.57	16.53	260	34,585	869	142,900
A300B2-100	2×51,000 lb (227 kN) GE CF6-50C turbofans	44.84	53.57	16.53	260	35,925	869	158,400
A300B4-200	2×52,500 lb (233.5 kN) CF6-50C1 turbofans	44.84	53.57	16.53	260	35,600	869	165,900
A310-202	2×48,000 lb (218 kN) GE CF6-80A turbofans	13.9	46.66	15.8	219	32,400	780	132,000

Table 2.9 (continued)

Type	Power plant	$S$ (m)	$L$ (m)	$H$ (m)	$A_w$ (m <sup>2</sup> )	$P_L$ (kg)	$V$ (km/h)	$W_a$ (kg)
(b) Antonov aircraft								
An-12	4 × 4000 ehp Ivchenko							
	A1-20 K turboprops	38	37	9.83	119.5	10,000	550	54,000
An-22	4 × 15000 ehp Kuznetsov							
	NK-12MA turboprops	64.4	57.8	12.53	345	80,000	679	250,000
An-24	2 × 2500 ehp Ivchenko							
	A1-24 Seviiny 11							
	turboprops	29.2	23.53	8.32	74.98	13,300	450	21,000
An~26*	2 × 2800 ehp Ivchenko							
	A1-24T turboprops	29.4	23.8	8.575	74.98	5500	435	24,000
An-28	2 × 970 ehp Glushenkov							
	TVD-10B turboprops	21.99	12.98	4.6	39.72	1550	350	6100
An-72	(similar to An-14)							
	2 × 14,330 1b (6500 kg)							
	Lotarev D-36							
	turbofans	25.8	26.58	8.24	74.98	7500	720	30,500

An-30 and An-32 have similar status to An-26

**Table 2.10** (a) Data for Boeing aircraft; (b) Data for the Ilyushin aircraft; and (c) Data for the Tupolev series of aircraft  
Service load parameters and stresses

Type	Power plant	<i>S</i> (m)	<i>L</i> (m)	<i>H</i> (m)	<i>A<sub>w</sub></i> (m <sup>2</sup> )	<i>P<sub>L</sub></i> (kg)	<i>V</i> (km/h)	<i>W<sub>a</sub></i> (kg)
(a) Data for Boeing aircraft								
727-200	3 × 16000 lb (71.2 kN) Pratt and Whitney JT8D-17 turbofans	32.9	461	10.4	153.2	18,594	883	95,238
737-200	2 × 16,000 lb (71.2 kN) Pratt and Whitney JT8D-17 turbofans	28.3	30.5	11.4	91	15,422	775	53,297
767	2 × 44,300 lb (1.97 kN) Pratt and Whitney JT9D-7R 4A turbofans	47.24	48.46	15.38	200	40,224	800	128,030
757	2 × 37400 lb (166.43 kN) Rolls-Royce RB211-535C turbofans	37.95	47.32	13.56	181.25	71,530	899	29,8880
747-200B	4 × 50,000 lb (222 kN) Pratt and Whitney JT9D-7F (wet) turbofans	59.6	70.5	19.3	512	71,530	907	366,500
747-200B	4 × 53,000 lb (236 kN) Pratt and Whitney JT9D-7Q turbofans	59.6	70.5	19.3	512	69,900	907	373,300
747-200B	4 × 52,500 lb (234 kN) General Electric CF6-50E2 turbofans	59.6	70.5	19.3	512	69,080	907	373,300
767-200B	4 × 52,500 lb (234 kN) General Electric turbofans	76.65	70.5	19.3	512	69,080	907	373,300

Table 2.10 (continued)

Service load parameters and stresses									
Type	Power plant	S (m)	L (m)	H (m)	A <sub>w</sub> (m <sup>2</sup> )	P <sub>L</sub> (kg)	V (km/h)	W <sub>a</sub> (kg)	
747-100B	CF6-50E2 turbofans								
	4 × 52,500 lb (234 kN)	65.0	70.71	19.18	512	69,080	907	373,300	
	General Electric CF6-50E2 turbofans								
(b) Data for Ilyushin aircraft									
	Ilyushin II-18								
	4 × Ivenchenko AI-20 M turboprops 4250ehp	37.4	35.9	10.17	140	14,000	625	64,000	
Ilyushin II-62	4 × 25,000 lb (113kN) Soloviev	43.2	53.1	12.4	280	23,000	860	165,000	
	20-30-KU turbofans								
	4 × Soloviev D.30KP turbofans. Each with 26,455 lb St (120,00 kg)	50.5	46.6	14.76	300	40,000	850	157,000	
Ilyushin II-86	4 × Kuznetsov turbofans, each with 28,635 lb St (13,000 kg)	48.06	59.5	15.81	320	42,000	900	206,000	
	2 × 21,385 lb (97 kN) Mikulin AM 3M500 turbojet	3454	25.85	11.9	174.4	900	800	76,000	
(c) Data for Tupolev aircraft									
	TU-124								
	2 × 11,905 lb (54 kN) Soloviev D-20P turbofans	25.5	30.58	8.08	1.19	3500	800	26,300	
TU-134	2 × 15,000 lb (66.5 kN) Soloviev D-30 turbofans	29	34.9	9	127	77,000	849	45,200	
	4 × 44,000 lb St (20,000 kg) with Kuznetsov NK-144 turbofans	28.8	6K7	12.85	438	14,000	2500	180,000	
TU-154)	3 × 21,000 lb (93.5kN) Kuznetsov NK-8-2 turbofans	37.5	48	11.4	202	20,000	900	91,000	

For 13767-200EH 46.55 48.46 16.155 For other details, reference is made to this Chapter  
For B747-400 65.00 70.71 19.18 For other details, reference is made to this Chapter

Table 2.11 Aircraft information Boeing 767-200ER

Aircraft information

Boeing 767-200ER

General specifications

<b>Passengers</b>	
Typical 3-class configuration	181
Typical 2-class configuration	224
Typical 1-class configuration	up to 255
<b>Cargo</b>	2,875 ft <sup>3</sup> (81.4)m <sup>3</sup>
<b>Engines' maximum thrust</b>	
Pratt & Whitney PW4062	£ 63,300 (28,713 kg)
General Electric CF6-80C2B7F	£ 62,100 (28,169 kg)
<b>Maximum fuel capacity</b>	23,980 U.S. gallons (90,770 liters)
<b>Maximum takeoff weight</b>	£ 395,000 (179,170 kg)
<b>Maximum range</b>	
6,600 nautical miles	
Typical city pairs: New York–Beijing	
12,200 km	
<b>Typical cruise speed at 33,000 ft</b>	
0.80 Mach	
530 mph (850 km/h)	
<b>Basic dimensions</b>	
Wing span	156 ft 1 in. (47.6 m)
Overall length	159 ft 2 in. (48.5 m)
Tail height	52 ft (15.8 m)
Interior cabin width	15 ft 6 in. (4.7 m)

FEDERAL EMERGENCY MANAGEMENT AGENCY

Service load parameters and stresses

Note: This aircraft has been used in the Twin Tower collapse.

Table 2.12 Military aircraft

Service load parameters and stresses		$S$ = span; $L$ = length; $H$ = height; $A_w$ = wing area; $P_L$ = payload $V$ = speed; $W_a$ = weight at takeoff or loading
Data on the Tornado IDS and ADV aircraft		
Power plant		
Interdictor Strike (IDS)		
Turbo-Union RB 199-34R (101 or 103) after burning turbofan MK 8090 lb (3670 kg) to 15,950 lb (7253 kg) after burning thrust		
$S$ (m)	8.60 max swept 13.90 max unswept	Air Defense Variant (ADV) As for IDS, with MK 104
$L$ (m)	16.67	
$H$ (m)	5.95	
$A \sim$ (m <sup>2</sup> )	.....	
$P_L \sim$ (kg)	9000	
$V$ (km/h)	Mach 2 at high level Mach 1 at low level	
$w_a$ (kg)	28,000	
Armament		
4 × MK 13/15 1000 lb (454.74 kg) bombs 2 AIM-9L missiles 8 MK 83 retarded bombs 2 CBLS-200 practice bomb containers 4 Kormoram ASM 8 × BL755 cluster bombs		
Basic parameters for the F-5E and F-20 aircraft		
Power plant		
Engine 2GEJ 85-21 Engine 5000 lb (2268 kg) thrust each		
$S$ (m)	7.98 with missiles 8.53 without missiles	GEF404-GE100 1800 lb (8164 kg) thrust each 8.5 with missile



Table 2.12 (continued)

Service load parameters and stresses		$S$ = span; $L$ = length; $H$ = height; $A_w$ = wing area; $P_L$ = payload $V$ = speed; $W_a$ = weight at takeoff or loading	
$L$ (m)	14.45		14.42
$H$ (in.)	4.07		4.10 (4.73 with wheels)
$A_w$ (m <sup>2</sup> )	28.1		27.5
$P_L$ (kg)	6350		7263
$V$ (miles/h)	850		1300
$W_a$ (kg)	11,213.8		12,700
Armament	Air-to-air 2 No. 20 mm guns and AIM 9 sidewinder missiles Air-to-ground 2 No. 20 mm guns and 9 bombs of 3020 kg		
Power plant	Data on the F-110 series		Data on the F-16 series of aircraft
	F-16A and F-16B	F-16C and F-16D	F-16 N
	Pratt and Whitney turbofan two shaft 24,000 lb (10,885 kg) thrust	F100-PW-200F100-PW-200 F110-GE-100 25,000 lb (11,340 kg) thrust	F110-GE-100 25,000 lb (11,340 kg) thrust
$S$ (m)	9.45	9.45	9.895
	10.01	10.01	(without sidewinder)
$L$ (m)	(with sidewinder)	(with sidewinder)	15.1
$H$ (m)	14.52	15.03	5.1
$A_{s^*}$ (m <sup>2</sup> )	5.01	5.09	27.87
$P_L$ (kg)	27.87	2787	37,500 lb (16,781 kg)
$V$ (mile/h)	33,000 lb (14,969 kg)	37,500 lb (16,781 kg)	1300
$W_a$ (kg)	1300	1300	17,278 lb (7836 kg)
	12,000 lb (5443 kg)	12,430 lb (5638 kg)	

**Table 2.13** (a) Data on the F-15; (b) data on the F/A-18 Hornet and (c) data for the Grumman F-14 Tomcat

Service load parameters and stresses		
(a) Data on F-15		Power plant
	2 No. Pratt and Whitney F-100-PW-220 each with 24,000 lb thrust	
$S$ (m)	13.05	
$L$ (m)	19.45	
$H$ (m)	5.64	
$A_w$ ( $m^2$ )	.....	
$P_L$ (kg)	7000	
$V$ (km/h)	2500	
$w_a$ (kg)	20,000	
Armament	4 AIM-9L/M infrared-guided Sidewinder missiles; 4 AIM-7F/M radar-guided Sparrow missiles; 8 advanced medium-range air-to-air missiles (AMRAAMs); M-61 20 mm Gatling gun with 940 rounds of ammunition. Accommodates a full range of air-to-ground ordnance	
(b) Data on F/A -18 Hornet		Power plant
	2 No. F404-UF <sup>+</sup> -400 Low bypass turbofan engines each in 1600 lb (70.53 kN) thrust and with a thrust/weight ratio of 8:1	
$S$ (m)	11.43	
$L$ (m)	17.06	
$H$ (m)	4.7	
$A_w$ ( $m^2$ )	37.2	
$P_L$ (kg)	.....	
$V$ (km/h)	2700	
$w_a$ (kg)	24,402	
Armament	Up to 7711 kg maximum on nine stations: two wing-tips for sidewinder heat-seeking missiles; two outboard wings for air-to-ground ordnance; two inboard wings for Sparrow radar-guided missiles, air-to-ground or fuel tanks; two nacelle fuselages for Sparrow missiles or sensor pods; one centreline for weapons, sensor pods or tank. Internal 20 mm cannon mounted in nose	
(c) Data on F-14 Tomcat		Power plant
	F-14A	F-14B, C
	2 × 20,900 lb (9480 kg) thrust Pratt and Whitney TF30-1412A	2 × 28,090 lb (12,741 kg) thrust Pratt and Whitney F401-400
$S$ (m)	Two shaft after-burning turbofans 11.630 (68° sweep) Safely landing 19.54 (20° sweep)	
$L$ (m)	18.89	
$H$ (m)	4.88	
$A_w$ ( $m^2$ )	.....	

**Table 2.13** (continued)

Service load parameters and stresses	
$P_L$ (kg)	17010
$V$ (km/h)	Mach 2.3 or 1564 mph maximum speed 400–500 km/h cruise speed
$w_a$ (kg)	27216
Armament	AIM-54 Phoenix missiles AIM-7 Sparrow missiles AIM-9 Sidewinder missiles

**Table 2.14** (a) Comparison data of MIG aircraft and (b) Data on the British Aerospace Jaguar

Service load parameters and stresses					
Power plant	MIG-19 (Mikoyan)	MIG-21	MIG-23 (Flogger)	MIG-25 (Foxbat)	MIG-27
Engines	Single seater 2×600 lb  (3040 kg)  to 2×7165 lb (3250 kg) Kimov RD-39B turbojets	Single seater Range turbojet 11,240 lb (5100 kg) 4150 lb (6600 kg) Tumanskey  single shaft	Single seater 17,640 lb  (8000 kg)  to 25,350 lb (11,500 kg)  thrust, 1 Tumansky turbofan	Single seater 27,000 lb  (12,250 kg)  thrust, 2 Tumansky R-266 after- burning turbojets	Single seater 17,640 lb  (800 kg)  to 25,350 lb (11,500) thrust, 1-  Tumansky after-burning turbofan
$S$ (m)	9	7.15	8.7 (72°sweep) 14.4 (16 sweep)	14 Foxbat A	8.7 (72°sweep) 14.4 (16 sweep)
$L$ (m)	13.08 (S-5F)	14.35	16.15	22.3 (Foxbat A) 22.7 (Foxbat R) 23.16 (Foxbat U)	16.5
$H$ (m)	4.02	4.5	3.96	5.6	4.6
$A_w$ (m <sup>2</sup> )	....	....	....	....	....
$P_L$ (kg)	3760	4600	7050	14,970	9900
$V$ (km/h)	Mach 1.3 or 1480 km/h (92 mph)	Mach 2.1 or 2070 km/h (1285mph)	Mach 1.1 or 1350 km/h (840 mph)	Mach 3.2 or 3380 km/h (2100 mph)	
$w_a$ (kg)	9500	9800	15,000	34,930	17,750

Table 2.14 (continued)

Service load parameters and stresses				
		Power plant		
		2 No. Rolls-Royce Terbomeca Adour two shaft turbofans		
		7305 lb (3313 kg) to 8000 lb (3630 kg)thrust		
$S$ (m)	8.69			
$L$ (m)	15.4–16.42			
$H$ (m)	4.92			
$A_w$ (m <sup>2</sup> )	.....			
$P_L$ (kg)	6800			
$V$ (km/h)	1450			
$w_a$ (kg)	1550			
Armament and other data	2 No. 30 mm DFA 553 each with 150 rounds			
	5 No. pylons with total external loads of 4536 kg with guns			
	2 No. 30 mm Aden for its T-2 model			
	Matra 550 Magic air-to-air missiles			
<i>Jaguar A and B and EMK 102 Audor engines</i>				
Jaguar S	MK 104s	} Audor engines	} Using digital quadruplex fly-by-wire control system	
	MK 108s			
Jaguar Act		}		
Jaguar FBW				

Jet Reaction ( $Y_r$ )

As a result of the postulated rupture of a high-energy system there develops an unbalanced differential pressure force plus a mass transfer momentum effect due to fluid being ejected from the rupture. In actuality an unbalanced external force develops on the system at each change in area and direction in the system. Typical reaction load characteristics due to a postulated rupture are given in the ANS N-176 guide.

Jet Impingement ( $Y_j$ )

As a result of a high-energy system rupture a high-energy fluid jet may form which would impinge on structures within its path. These structures in general would be designed 4o resist the momentum transfer resulting from the structure stopping the jet.

Reaction Load Due to Accident-Induced Differential Movement ( $R_a$ )

Many structures and components are supported by primary structures which would undergo deformation from an accident condition and thereby induce loads in the supported structure or component. Examples of this effect would be loads on piping systems attached to the containment, which would be induced when the containment expands due to accident pressure and temperature effects.



Table 2.16 Comparative data of some important combat aircraft

Type	Power plant	S (m)	L (m)	H (m)	P <sub>L</sub> (kg)	V (km/h)	w <sub>a</sub> (kg)
BAe Harrier	1 × 21,500 lb (9752 kg) thrust	7.7	13.87	3.43	6200	1.2	11,793
GR-3 model T-Mark 4 model (AV-8A, TAV-8A) FRS-I model Single-seater, two-seater	Rolls-Royce Pegasus 103 two shaft turbofan (US designation F-400)		17.0 (GR-3)				
F-6 Shenyang (or NATO's name FANTAN 'A')	2x Axial turbojets	10.2	15.25	3.35	4500	1	10,700
Single seater	MD manufactured					760	
Rockwell B-1	4 × 30,000 lb (13,610 kg)	41.4	45.6	10.24	11,5670	0.85	179,170
Four seater	General Electric F101-100 two shaft augmented turbofans						
Saab 37 AJ, JA	1 Svenska flying motor RMB;	10.6	AJ: 10.6 JA: 16.3	5.6	4500	2	16,000
Viggen SF, SH, SK versions	Pratt and Whitney two shaft 25,970 lb (11,790 kg) to 28,086 lb					1320	
Single seater	(12,750 kg) thrust	8.43	SU-9: 18.5 SU-11: 17.4	4.9	4540	0.95	13,610
SU-9 Fishpot B Fishpot C	1 Lyulka single shaft turbojet; 19,840 lb (9000 kg) thrust (SU-9) and 22,040 lb (10,000 kg) thrust (SU-11)					1195	
Single seater	2x Tumonsky R-25 turhofans; 16,530 lb (7500 kg) thrust after burner (17)	9.5 D model	21.5	5	10,100 D 5100 A	2.3 1520	21,000 D 16,000 A
SU-15 (Flagen A to E models)							
Single seater	1-Lyulka AL-21 F-3	14 (28° sweep) 10.6 (62° sweep)	18.75	4.75	9000	1.05 798	19,000
SU-17, SU-20 and SU-22 models	Thrust single shaft 17,200 lb (7800 kg) (20-22) AL-7F					To	2.17
Single seater	22,046 lb (10,000 kg)					1432	

Table 2.17 Types of shells, bombs, rifles

Service load parameters and stresses			
Types of shells and bombs	Manufacturers	Dimensions	$w_L$ (kg)
Double base	International	$d=1.25$	...
Shot gun		$t=0.150$	...
Single or double	International	$d=0.875$	...
base rim fire		$t=0.1$	...
Double base	International	$d=1$	...
revolver		$t=0.125$	...
Single base rifle	International	$d=1.25$	...
		$d=0.375$	...
		$t=0.045$	...
GBU-15	Rockwell	$L=3.75$	MK84
HOBOS-guided	International	MK84	2240
bomb	USA	$S=112$	1016
		$d=46$	M118
		(M118)	3404
		$S=132$	
		$d=61$	
Bofor	Sweden	....	0.12
			5500 kg guns
ZSU-23-4	USSR	$L=654$	20.5
		$d=29.5$	SPAA vehicles 4×3
		3400 rounds	automatic
GBU-15(V)2	USA	$L=388$	
glide bomb			Imaging infrared
(smart bomb)			Short

$d$  = diameter (mm);  $t$  = web thickness (mm);  $L$  = length (cm);  
 $w_L$  = weight;  $S$  = span (cm);  $R$  = distance;  $V$  = velocity

Medium

....

....

Short

....

Short

....

Short

....

Short

....

Short

....

Short

....

Short

....

Short

....

Short

....

Short

....

Short

....

Short

....

Short

....

Short

....

Short

....

Short

....

Short

....

Short

....

Short

....

Short

....

Short

....

Short

....

Short

....

Short

....

Short

....

Short

....

Short

....

Short

....

Short

....

Short

....

Short

....

Short

....

Short

....

Short

....

Short

....

Short

....

Short

....

Short

....

Short

....

Short

....

Short

....

Short

....

Short

....

Short

....

Short

....

Short

....

Short

....

Short

....

Short

....

Short

....

Short

....

Short

....

Short

....

Short

....

Short

....

Short

....

Short

....

Short

....

Short

....

Short

....

Short

....

Short

....

Short

....

Short

....

Short

....

Short

....

Short

....

Short

....

Short

....

Short

....

Short

....

Short

....

Short

....

Short

....

Short

....

Short

....

Short

....

Short

....

Short

....

Short

....

Short

....

Short

....

Short

....

Short

....

Short

....

Short

....

Short

....

Short

....

Short

....

Short

....

Short

....

Short

....

Short

....

Short

....

Short

....

Short

....

Short

....

Short

....

Short

....

Short

....

Short

....

Short

....

Short

....

Short

....

Table 2.18 Missiles for armed forces (ICBM and ALCM) (USA, USSR)

Service load parameters									
Types of missiles/rockets	Manufacturer/ country of manufacture	Dimensions	WL lb (kg)	Power plant and guidance	R miles (km)	V mach	Warhead manufacture	Mechanisms	
								Thermo	B-52
AGM-86A air-launched cruise missile (ALCM)	Boeing,	$L = 4.27$	1900	Williams Research F107-	760	0.6–0.8	Thermo nuclear		
	Aerospace, Seattle, USA	$S = 289$ $d = 64$	862	WR-100 2. No shaft thrust; McDonnell Douglas	1200	200 kt			
LGM-30	Boeing	$L = 18.2$	Model III	Tercom with inertial system					
				I-Stage: Triokol TU-120	II stage:	1500 mph	Thermo nuclear		SG
Minuteman (ICBM) missile, located in silos	Aerospace, Ogden, USA	$d = 183$	70,116	(M55E), $2 \times 10^5$ lb	7000		1–5 Mt		
			31,800	( $9 \times 10^5$ kg) thrust	11,250		II stage:		
			Model III	II Stage: Hercules rocket	III stage:				
			76,015	$35 \times 40^3$ lb ( $16 \times 3$ kg)	8000		AVCO MK		
RS-121SS13	USSR	–	34,475	thrust	12,875		IIC		
				III-Stage: Aerojet $35 \times 10^3$ lb ( $16 \times 10^3$ kg) thrust			III stage: GE MK-12 MIRV		
Savage (ICBM) RS-16/SSI7 (ICBM)	USSR	–	–	Solid fuel propellant; three stages	9400	0.8	Nuclear 75 kt		SG
				Liquid cold launch; two stages	11,000	0.8	3.6 Mt mode 2 or MIRV		SG
					1000		$4 \times 200$ kt		



Table 2.18 (continued)

Service load parameters								
Manufacturer/ country of manufacture		Dimensions	WL lb (kg)	Power plant and guidance	R miles (km)	V mach	Warhead manufacture	Mechanisms
Types of missiles/rockets								
RS-20/SS18	USSR			Liquid propellant; two stages	10,000	1	5-10Mt	
(ICBM)							mode 2	
SS-23 Scalpel	USSR	–	–	Solid cold launch propellant; three stages	10,000	1	Nuclear MIRV	Rail
(ICBM)							8–10x	mobile
SS-25 Sickle	USSR	–	–	Solid cold launch propellant; three stages	10,500	1	Nuclear 550 kt	
(IRBM)								

Table 2.19 Missiles for armed forces (BGM, M, MK, RGM, etc.) (USA, France, Israel)

TOW 2 (BGM-71 D)	USA	$L = 140$ $d = 15$	21.5	Solid propulsion; wire manual or auto	3.75	Heat conventional	SSM anti-tank
Copperhead (M712)	USA	$L = 137$ $d = 15$	63.5	Cannon launched: laser homing	16	Heat 6.4 kg	SSM anti-tank
Gabriel	Israel	$L$	$S$ $d$	Two-stage solid propulsion; auto pilot/command	18	Conventional 100 kg	SSM anti-tank
MK I		335	135 34		36	100 kg	SSM shipborne
MK II		341	135 34		36+	100 kg	
MK III		381	135 34		200	150 kg	
MK IV		381	135 34	Turbojet propulsion: inertial and active radar homing			
SS-N-3	USSR	$L = 1020$	4700	Solid boosters: internal turbojet radio command	460–735	Nuclear and Conventional	SSM shipborne
Shaddock		$d = 86$					
(SRM)							
Harpoon	USA	$L = 384$	519	Solid booster turbojet cruise: inertial and radar	90	Conventional	SSM
(RGM-84A)		$S = 830$ $d = 34$					shipborne
Deadeye 5	USA	$L = 384$ $d = 12.7$	47.5	Solid propulsion; laser homing	24	–	Guided projectile; shipborne
Crotale	France	$L = 290$ $S = 54$ $d = 15$	80	Solid propulsion: radio command	18	15 kg conventional	NSA
Sadral	France	$L = 180$ $d = 16$	17	Solid propulsion; infrared homing	0.3–6	3 kg heat conventional	NSA

Table 2.20 Data and parameters on missile types

Service load parameters and stresses							
Barak missile	Israel Aircraft Industries (IAI)	$L = 217$ $d = 17$	86 –	Semi-active radar-homing missile with disposable launch canister, manually fitted to an 8-round launcher based on the MBT TCM-30 twin 30 mm anti-aircraft gun mounted	10	Conventional 2 nuclear 7 kg	NSA small patrol boats
SA-N-3	USSR	$L = 620$	550	Solid propulsion: semi-active homing semi-active homing	55	80 kg conventional	NSA
Goblet		$S = 150$ $d = 33.5$					
SA-N-4	USSR	$L = 320$	190	Solid propulsion: semi-active homing semi-active homing Solid propulsion and command	14.8	50 kg	NSA
Roland 3	France and Italy	$d = 21$ $L = 260$	85		8	9 kg conventional	ADM
SA-4 Gancf	USSR	$S = 50$ $d = 27$ $L = 880$	100,000	Ramjet and solid boosters; radio command	70	135 kg	ADM
(SRM)							
SA-10 Grumble MMIO	USSR	$S = 290$ $L = 700$	1500	Solid propulsion	100	Nuclear	ADM
		$S = 10$ $d = 45$					
SA-12 Gladiator	USSR	$L = 50$ $S = 350$ $d = 50$	2000	Solid propulsion: semi-active radar	80	150 kg conventional	ADM

Table 2.20 (continued)

Service load parameters and stresses							
SA-13 Gopher (HJ-8)	USSR	$L = 220$	55	Solid propulsion: infra—red homing infrared homing	10	4 kg	ADM
		$S = 40$ $d = 12$				conventional	
BGM-109	General	$L = 5.56$	2200	Williams Research F 107	1 727	0.72	Thermo- nuclear nuclear SG
Tomahawk cruise missile	Dynamics	$S = 2.45$	1000	Turbofan 600 lb (272 kg)	2780	(550 mph/ 885 km/h)	
(IRBM)	Convair, San Diego, USA	$d = 0.53$	to 4000 1814	Thrust guidance MD Tercom and inertial			1000 lb (454 kg)
CSS-2	China	—	—	Liquid propellant Stage 2	120,00	0.8	Nuclear 2 Mt SG
CSS-3				Stage 3			1–5 Mt
(IRBM)				Liquid propellant	1200	0.7	Nuclear 20 kt SG
CSS-1	China	—	—	Two stages	2700		1–3 Mt 1 Mt
CSS-2				Two stages	2000		
(IRBM)							
Sandal	—	—	—	Solid propellant	3000	0.65	Nuclear 1.2 Mt
(IRBM)	France	—		Two stages	3000	0.65	Nuclear 1.2 Mt
SSBS S-3	USSR	—		Solid propellant	3000	0.65	Nuclear 1.2 Mt
SS-N-20							
Sturgeon							
(IRBM)							

Table 2.20 (continued)

Service load parameters and stresses							
UGM-73	Lock heed	$L = 10.36$	65000	Solid motor Thiokol as first stage; Hercules as second stage; guidance: inertial	3230	10	Lockheed
Poseidon missile (IRBM)	Missiles and Space Company, California, USA	$d = 1.88$	-29500		5200		MIRV carrying 50 kt Rvs
UGM-27	Lockheed, USA	$L = 9.45$	35000	Aerojet solid motor with jetavator control as first stage; Hercules motor missile with liquid injection as second stage	2875	10	MIRV Submarine
Polaris (ICBM)	California, USA	$d = 1.37$	-15850		(4631)		200 kt launch

Table 2.21 Missiles and rockets

Service load parameters and stresses			w <sub>L</sub> (lb)	Power plant and guidance	R (km)	Warhead	Mechanisms
Type of missile/rockets	Manufacturer/country of manufacture	Dimensions					
Blood hound	UK	L = 846 S = 283 d = 55		Ramjet and solid boosters; semi-active radar homing	80	Conventional	ADM
Blow pipe	UK	L = 139 S = 270	20.7	Solid propulsion; radio command	Any short distance		
Javelin	UK	L = 40 d = 8		Solid propulsion; Saclos	3 4 +	Conventional	ADM shoulder-fixed ADM
Hawk MIM-23B	USA	L = 503 S = 119 d = 36	627.3	Solid propulsion; semi-active Homing	40	Conventional	ADM
Stinger FIM-92A	USA	L = 152 S = 14 d = 7	15.8	Solid propulsion; infrared homing	Short range 3	Conventional	ADM
MIM Hercules L-5B	USA China	L = 1210 d = 80 L = 289 S = 66 d = 13	4858 85	Solid propulsion; command Solid propulsion; infrared	140 5	Nuclear and conventional Conventional	ADM AAM
L-7	China	L = 25 S = 66 d = 16	90	Solid propulsion; infrared	5	Conventional	AAM
Mistrel	France	L = 180 d = 9	18	Solid propulsion; infrared	3	3 kg conventional	AAM
Super 530	France	L = 354	250	Solid propulsion	25	3 kg	AAM

Table 2.21 (continued)

Service load parameters and stresses			Dimensions	$w_L$ (lb)	Power plant and guidance	$R$ (km)	Warhead	Mechanisms
Type of missile/rockets	Manufacturer/country of manufacture							
M Type (SRM)	China		$L = 910$	6200	Solid propulsion; inertial	600	Nuclear	SSM
Frog-7 (SRM)	France		$L = 910$ $d = 85$	2300	Solid propulsion	70	Nuclear	SSM
SS-IC Scud B	USSR		$L = 1125$ $d = 85$	6370	Storable liquid; inertial	280	Nuclear	
SS-23 Spider (SRM)	USSR		$L = 605$ $d = 100$	3500	Solid propulsion; inertial	525 miles	Nuclear	SSM
Exocet MM10	France		$L = 578$ $S = 100$ $d = 35$	850	Solid propulsion; two stages: inertial and active radar Homing	70	165 kg Conventional	SSM ship
RBS 15	Sweden		$L = 435$ $d = 50$	600	Turbojet boosters	150	Conventional	SSM ship
Arrow 8(Hj-8)	China		$L = 99.8$ $S = 47$ $d = 10.2$	11.3	Solid propulsion; wire guided	0.1–3	Heat	SSM antitank
Spandrel	USSR		$L = 100$ $d = 16$	12–18	Solid propulsion; semi-automatic	4	Heat	SSM antitank
Vigilant	UK		$L = 107$ $S = 28$ $d = 11$	14	Solid propulsion; two stages: wire manual or auto	1.375	Heat 6 kg	
Dragon 1M47	USA		$L = 74$ $S = 33$ $d = 13$	13.8	Multiple solid propulsion; wire manual	1	Heat	SSM antitank

Table 2.22 Missiles with warhead mechanisms

Service load parameters and stresses										
Types of missiles/rockets	Manufacturer/ country of manufacture	Dimensions			$w_L$ lb (kg)	Power plant and guidance	$R$	$V_{mach}$ (mph)	Warhead	Mechanisms
		$L$	$S$	$d$						
C-601	China	738	280	92	2440	Liquid propulsion	100 km	–	400 kg	ASM
HY-4		736	280	7.6	1740	Turbofan propulsion	150 km	–	to 500 kg	ASM
C-801		480	165	55	1025	Solid propulsion All active radar	150 km	–	Conventional	ASM
S-9	USSR	$L$	$S$	$d$	750	Solid propulsion:	150 km	–	Conventional	ASM
S-10		600	150	50	300	semi-active laser	300 km min	–	Conventional	ASM
AS-II	USSR	$L = 350$	$S = 90$	$d = 30$	300	Solid propulsion: infrared	110 km	–	Conventional	ASM
Sea Eagle		$L = 414$	$S = 120$	$d = 40$	600	Turbofan inertial: active radar	8 miles	6–10	Mk 19 113 kg	ASM
AGM-65		$L = 246$			462 (210)	Thiokol TX-481 solid motor: AGM-65C laser guidance	(13 km) to 14 miles (22.5 km)	200	Conventional	ASM
Maverick	Aircraft, Tulson, USA	$S = 71$	$d = 44.5$			LPC (Lockheed Company)	High 105 miles (170 km): low 35 miles (56 km)		Nuclear	Rocket
AGM-69A SRAM	Boeing	$L = 4127$			2230	Propulsion two-pulse solid motor: guidance: inertial			170 kT	
	Aerospace, Seattle,	$S = 89$	$d = 44.5$		1010					



Table 2.22 (continued)

Service load parameters and stresses								
Types of missiles/rockets	Manufacturer/ country of manufacture	Dimensions	$w_L$ lb (kg)	Power plant and guidance	$R$	$V_{mach}$ (mph)	Warhead	Mechanisms
USA								
ASLAM	McDonnell Douglas, USA	$L = 4127$	2700	Internal rocket		6–10	170 kt nuclear and conventional	ASM
Missile MK III		$S = 89$	1200	ramjet: guidance: inertial with Tercom				
MK IV		$d = 44.5$						
Types of missiles/rockets	Manufacturer/country of manufacture	Dimensions		$w_L$ lb (kg)	Power plant and guidance	$R$	Warhead	Mechanisms
550 Magic	France	$L = 275$ $S = 66$ $d = 16$			Solid propulsion; Infrared	5 km	Conventional	AAM
AIM-9	Naval	$L = 283$ –		Up to	Rocket dyne, Thiokol,	2.5 + miles	XM 248	AAM
Sidewinder	Weapon Centre,	2.91	190		Bermite or Naval	cruise	high explosive	(F-16, F-20,
	Philco-Ford	$S = 56$ –	86		propellant;	6 miles	(150 lb)	F-5E aircraft)
	Ford Aero-space	64 $d = 12.7$			Single Grain solid MK 17, 36, 86; guidance: 9E to 9L, high power servo-system, AM/	max		
	General Electric							

Table 2.22 (continued)

Types of missiles/rockets	Manufacturer/country of manufacture	Dimensions	$w_L$ , lb (kg)	Power plant and guidance	$R$	Warhead	Mechanisms
	USA			FM IR conical scan head or Raytheon track			
Alamo AA-10	USSR	$L = 400$ $S = 70$ $d = 19$	200	via missile Solid propulsion; semi-active or infrared	30 km	Conventional	AAM
AMBAAM	USA	$L = 357$  $S = 63$ $d = 18$	150	Solid propulsion; command and inertial	12 km	Conventional	AAM
Falcon	USA	$L = 213$ $S = 639$ $d = 29$	115	Solid propulsion; semi-active radar	8 km	Conventional	AAM
Phoenix	USA	$L = 396$ $S = 92$ $d = 38$	454	Solid propulsion; semi-active radar	150 km	Conventional	AAM
Sparrow AIM-7 M	USA	$L = 366$ $S = 102$ $d = 20$	227	Solid propulsion; infrared	140 km	Conventional	AAM

$L$  = length (cm),  $S$  = wingspan (cm),  $d$  = diameter (cm),  $W_L$  = launch weight,  $R$  = range

**Table 2.23** Missiles for armed forces (ADM and NSA types) (UK, USA)

Table 2.23 (continued)

Service load parameters and stresses						
Types of missiles/rockets	Manufacturer/ country of manufacture	Dimensions	$w_L$ lb (kg)	Power plantand guidance	$R$ miles (km)	$V$ mach (mph)
Sea Dart Missile	British	$L = 4.4$ $d = 42$	550	Marconi radar	30	—
	Aerospace, UK			805 SW tracker with type 909 illuminator; guidance: semi		
Sea Wolf Missile	British Aerospace, UK	$L = 1.9$ $d = 18$	82	GWS 25 — Marconi radar (805547) search, tracking radars, Ferranti fire-control computer; guidance: radio command	30	—
Sea Cat Missile	Short Brothers, Belfast, UK	$L = 1.47$ $d = 19$	63	Radio command guidance with optical remote TV and radar- aided tracking	30	—
Raytheon/ Martin XMIM- 104A Patriot missile	Martin Orlando Division, USA	$L = 5.31$ $S = 87$ $d = 41$	3740 1696	Thiokol TX-486 single-thrust solid motor	30 48	3–5 Advanced mobile system SAM

$L$  = length (cm),  $S$  = wingspan (cm),  $d$  = diameter (cm),  $W_L$  = launch weight,  $R$  = range,  $V$  = speed

## Helicopters

Helicopters are more vulnerable than aircraft in warfare. In peace time a helicopter may crash after losing a rotor or hitting objects such as offshore platforms, buildings, helipads or their surrounding structures. Table 73 gives useful data for some types of helicopters in the book “Shock, Impact and Explosion” by the authors published by Springer-Verlag (Germany) 2008.

### 2.2.3.7 Load Combinations

Based on American Standards

#### *Load Combinations for Concrete Structures*

Design load combinations for concrete structures are given in the following two industry standards, depending on the type of structure being designed.

1. Code for Concrete Reactor Vessels and Containments –ASME Section III, Division 2 and ACI 359-77. Prepared by Joint ACI-ASME Technical Committee on Concrete Pressure Components for Nuclear Service.
2. Standard for Design of Concrete Structures in Nuclear Service other than Pressure Retaining Components ACI-349.

The loading equations found in these industry standards may not agree with NRC published guidelines. In such cases the designer should be assured the load combinations used are acceptable to the regulatory authorities.

3. Load Combinations for Steel Structures –For steel structures, a definitive industry standard (ANSI N690) is still used. In general, load combinations are acceptable if they are found in accordance with the following
4. For service load conditions, either the elastic analysis working stress design (WSD) methods of Part 1 of the AISC Specification or the plastic (limit) analysis load factor design (LRFD) methods of Part 2 of the AISC Specification may be used.

If the elastic analysis WFD methods are used, the following load combinations should be considered:

1.  $D + L$
2.  $D + L + E_0$
3.  $D + L + W$

If thermal stresses due to  $T_0$  and  $R$  are present, the following combinations should also be considered:

- 1a.  $D + L + T_a + R_0$
- 2a.  $D + L + T_0 + R_0 + E_0$
- 3a.  $D + L + T_0 + R_0 + W$

Both cases of  $L$  having its full value or being completely absent should be checked.

If plastic (limit) analysis LRFD methods are used, the following load combinations should be considered:

1.  $1.7D + 1.7L$
2.  $1.7D + 1.7L + 1.7E_0$
3.  $1.7D + 1.7L + 1.7W$

If thermal stresses due to  $T_0$  and  $R_0$  are present, the following combinations should also be considered:

- 1b.  $1.3(D + L + T_0 + R_0)$
- 2b.  $1.3(D + L + E_0 + T_0 + R_0)$
- 3b.  $1.3(D + L + W + T_0 + R_0)$

Both cases of  $L$  having its full value or being completely absent should be checked.

For factored load conditions which represent extreme loads the following load combinations should be considered:

Elastic analysis WSD methods are used:

4.  $D + L + T_0 + R_0 + E_{ss}^1$
5.  $D + L + T_0 + R_0 + W_t$
6.  $D + L + T_a + R_a + P_a$
7.  $D + L + T_a + R_a + P_a + 10(Y_j + Y_r + Y_m) + E_0$
8.  $D + L + T_a + R_a + P_a + 10(Y_j + Y_r + Y_m) + E_{ss}^1$

If plastic (limit) analysis LRFD methods are used:

4.  $D + L + T_0 + R_0 + E_{ss}^1$
5.  $D + L + T_0 + R_0 + W_t$
6.  $D + L + T_a + R_a + 1.5P_a$
7.  $D + L + T_a + R_a + 1.25P_a + 1.0(Y_j + Y_r + Y_m) + 1.25E_a$
8.  $D + T_a + R_a + 1.0P_a + 1.0(Y_j + Y_r + Y_m) + 1.25E_{ss}^1$

## European Codes

The most important codes indulging in nuclear facilities are EC2, EC3, EC8, EC9, etc. It is extremely difficult to specifically assign combination for nuclear facility. The best possible combination can be given after examining various design practices in Europe where European codes are used, all loads can be calculated using respective codes. The following combinations of various loads are given below:

$$\begin{aligned}
 U &= 1.4D + 1.7L \\
 U &= 0.75(1.4D + 1.7L \pm 1.87E) \\
 U &= 0.75(1.4D + 1.7L \pm 1.7W) \\
 U &= 0.9D \pm 1.43E \\
 U &= 0.9D \pm 1.3W \\
 U &= 1.4D + 1.7L + L^7 H_{mep}
 \end{aligned}$$

$$U = 0.9D + 1.7H$$

$$U = 0.75(1.4D + 1.4T_d + 1.7L)$$

$$U = 1.4(D + T_d)$$

For reinforced concrete the following modifications are introduced where earthquakes are involved:

$$U = 1.4(D + L \pm E)$$

$$U = 0.9D \pm 1.4E$$

where  $U$  = required strength to resist factored loads or related internal moments and forces;  $D$  = dead loads or related internal moments and forces;  $L$  = live loads or related internal moments and forces;  $W$  = wind loads or related internal moments and forces;  $E$  = load effects of earthquake or related moments and forces;  $T_d$  = internal moments and forces due to differential settlement, creep, shrinkage or temperature effects;  $H_{mep}$  = moments or forces due to earth pressure.

Loads computed from the Euro codes can still be combined using American practices given above. Care should be taken that all industrial concerns have been consulted and approvals are obtained for the design of various structural elements of nuclear facilities.

## 2.3 Determination of Impulse/Impact caused by Aircraft and Missiles: Load ( $I$ )

### 2.3.1 General

An impactor in the form of an aircraft or a missile develops from initial velocity to a velocity caused by its movement under the action of its own weight or a booster's force. In any circumstances, if the kind of velocity is not vertical it will move in a curve and its flight can be evaluated in terms of horizontal and vertical components of displacement, velocity and acceleration. Alternatively, the directions are controlled in any specific direction from the control centre.

#### 2.3.1.1 Direct Impulse/Impact and Momentum

An impulse is defined as a force multiplied by time, such that

$$F_1(t) = \int F dt \quad (2.1)$$

where  $F_1(t)$  is the impulse,  $F$  is the force and  $t$  is the time. The momentum of a body is the product of its mass and its velocity:

$$\text{Momentum} = mv \quad (2.2)$$

where  $m$  is the mass and  $v$  is the velocity  $= dx/dt$ . Both velocity and momentum are vector quantities; their directions are the same. If a body is moving with a

constant velocity, its momentum is constant. If velocity is to be changed, a force  $F$  must act on the body. It follows that a force  $F$  must act in order to change the momentum.

$$F = mdv/dt \quad (2.2a)$$

or

$$Fdt = mdv$$

Integrating both sides

$$\int_{t_1}^{t_2} = \int_u^v mdv \quad (2.3)$$

$$F_1(t) = m(v - u)$$

where  $u$  and  $v$  are the velocities at times  $t_1$  and  $t_2$ , respectively. If the initial velocity  $u = 0$ , Eq. (2.3) becomes

$$I = mv \quad (2.3a)$$

Thus the impulse of a force is equal to the change in momentum which it produces.

### 2.3.1.2 Impacts/Collisions of Aircraft

When two solid aircraft are in contact, they exert equal and opposite forces or impulses on each other and they are in contact for the same time. If no external force affects the motion, the total momentum in the specific direction remains constant. This is known as the *principle of conservation of linear momentum*. When two aircraft  $m_1$  and  $m_2$ , collide (Fig. 2.1), the mass ratios are then calculated from Eq. (2.1):

$$F_{11}(t) = m_1(v_1 - u_1) = \int F_1 dt \quad (2.4)$$

$$F_{12}(t) = m(v_2 - u_2) = \int F_2 dt$$

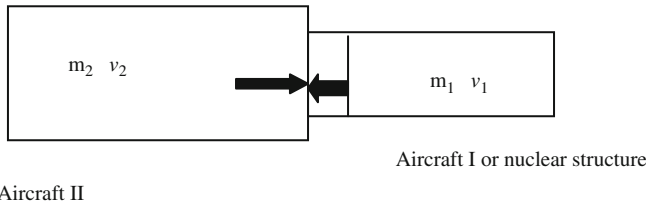


**Fig. 2.1** Direct impact



Since  $\int F_1 dt = \int F_2 dt = 0$ , the relationship between the velocity change and mass becomes

$$m_2/m_1 = (v_1 u_1)/(v_2 - u_2) \quad (2.5)$$

During the collision process, although the momentum is conserved, there is a loss of energy on impact which is determined using the concept of the *coefficient of restitution*,  $e$ , which is defined as the relative velocity of the two masses after impact divided by the relative velocity of the two masses before impact. Before impact

$$e = (v_1 - v_2)/-(u_1 - u_2) = 0$$

When the relative velocity vanishes, and

$$e = (v_1 - v_2)/-(u_1 - u_2) = 1 \quad (2.5a)$$

there is no loss of relative velocity.

Where  $e < 1$ , it is related to the loss in kinetic energy, and where  $u_2 = 0$  (refer to Eq. (2.5a))

$$\begin{aligned} m_1(v_1 - u_1) + m_2(v_2) &= 0 \\ v_1 - v_2 &= eu_1 \end{aligned} \quad (2.6)$$

Hence

$$v_1 = u_1(m_1 - em_2)/(m_1 + m_2) \quad (2.6a)$$

$$v_2 = u_1[(1 + e)m_1/(m_1 + m_2)] \quad (2.6b)$$

The original kinetic energy  $(KE)' = \frac{1}{2}m_1 u_1^2$

The final kinetic energy  $(KE)'' = \frac{1}{2}(m_1 v_1^2 + m_2 v_2^2)$

$$(KE)' - (KE)'' = \frac{1}{2}m_1 u_1^2 - \frac{1}{2}(m_1 v_1^2 + m_2 v_2^2) \quad (2.7)$$

Substituting the values of  $v_1$  and  $v_2$

$$(KE)' - (KE)'' = (KE)'[m_1(1 - e^2)/(m_1 + m_2)] \quad (2.8)$$

The displacement resulting from a short-duration ( $\tau$ ) impact is given by

$$x = b(t - \tau) \quad (2.9)$$

where  $t$  is the time beyond  $\tau$ . For dynamic analysis, the impact time is divided into  $ns$  small segments and, using Eq. (2.3a),

$$\begin{aligned} x &= \frac{1}{m} \sum_0^n v_n I_n(t - \tau_n) \\ &= \frac{1}{m} \int_0^t F(t - \tau) d\tau \end{aligned} \quad (2.10)$$

The impact is divided into two phases such that in the first, from time  $t_1$  to  $t_0$ , there will be compression and distortion until  $(v_1 + v_2)$  are both reduced to zero (the both aircrafts moving together); in the second, the elastic strain energies in the aircraft are restored and are separated by a negative velocity,  $-V_2 = (v_1 + v_2)$ .

During the second phase the impulse relation between the aircraft  $(F_T - F_{T0})$  will be proportional to  $F_{T0}$  and the coefficient or restitution  $e$  defined above is written as

$$e = (F_T - F_{T0})/F_{T0} \quad (2.11)$$

where  $F_T$  is the total impulse during the impact and  $F_{T0}$  is the impulse in phase one.

At time  $t_0$

$$V_0 = v_{10} + v_{20} = v_1 + \left( \frac{F_{T0}}{m_1} + v_2 - \frac{F_{T0}}{m_2} \right) = 0 \quad (2.12)$$

hence

$$V = v_1 + v_2 = \left( \frac{1}{m_1} + \frac{1}{m_2} \right) F_{T0} \quad (2.13)$$

Similarly, at time  $t_2$  the relationship becomes

$$V_0 - V_2 = F_T \left( \frac{1}{m_1} + \frac{1}{m_2} \right) \quad (2.14)$$

Using Eq. (2.11), the expression given in Eq. (2.5a) may be written in the form

$$-\frac{V_2}{V} e \quad (2.15)$$

Equations (2.6), (2.6a) (2.6b) result from the above method. However, from Eq. (2.11) the total impulse is rewritten as

$$F_T = \left( \frac{m_1 m_2}{m_1 + m_2} \right) (1 + e)(v_1 + v_2) \quad (2.16)$$

$$M(1 + e)V$$

where  $M$  is the equivalent combined mass of the aircrafts.

The changes in velocity after impact of the aircrafts are written as

$$\begin{aligned}\Delta V_1 &= \frac{M}{m_1}(1+e)(v_1 + v_2) = \frac{M}{m_2}(1+e)V \\ \Delta V_2 &= \frac{M}{m_2}(1+e)V\end{aligned}\quad (2.17)$$

### 2.3.1.3 Oblique Impact

When two aircraft collide and their axes do not coincide, the problem becomes more complex. With oblique impact, as shown in Fig. 2.2, two impulses are generated: the direct impulse,  $F_T$ , and the tangential impulse,  $F'_T$ . The latter is caused by friction between the impacting surfaces and by local interlocking of the two aircraft in the common surface. Let the angular velocity of the two aircraft be  $\theta_1$  and  $\theta_2$ , respectively. If  $F'_T/F_T = \lambda'$  and the body's centre of gravity has a coordinate system  $X$  and  $Y$ , the components of the vector velocity,  $v_1$  and  $u_1$ , normal to the impact surface may be written as follows:

$x_1 - y_1$  system

$$v_1 = |\bar{v}_1| \cos \theta_1 \quad (2.18)$$

$$u = |\bar{v}_1| \sin \theta_1 \quad (2.18a)$$

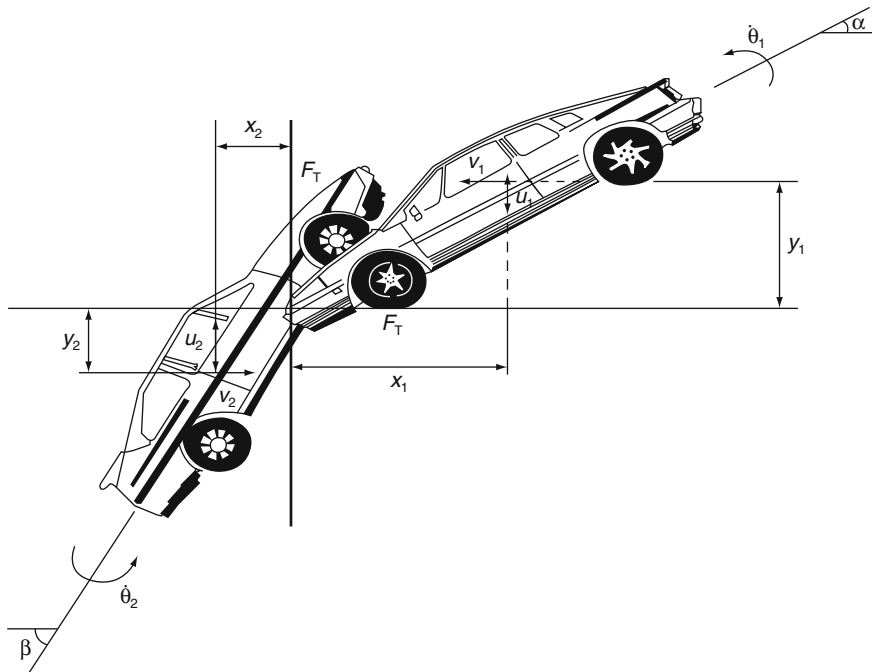


Fig. 2.2 Oblique impact of the bodies of two different objects

Similarly,  $v_2$  is written as

$$|\bar{v}_2| = V(v_2^2 + u_2^2) \quad (2.19)$$

$$\beta = \tan^{-1}(u_2/v_2) \quad (2.19a)$$

The momentum equations for the bodies are summarised below:

$$\left. \begin{aligned} m_1 v'_1 - F_T &= m_1 v'_2 \\ m_1 u'_1 - \lambda' F_T &= m_1 u'_2 \\ m_1 R^2_1 \theta'_1 + F_T y_1 - \lambda' F_T x_1 &= m_1 R^2_1 \theta'_2 \end{aligned} \right\} \quad \begin{array}{l} \text{body 1} \\ (2.20) \end{array}$$

where  $v'_1, v'_2, u'_1$  and  $u'_2$  are for  $t_1$  and  $t_2$ .

$x_2 - y_2$  system

$$\left. \begin{aligned} m_2 v''_1 - F_T &= m_2 v''_2 \\ m_2 u''_1 - \lambda' F_T &= m_1 u'_2 \\ m_2 R^2_2 \theta'_2 + F_T y_2 - \lambda' F_T x_2 &= m_2 R^2_2 \theta'_2 \end{aligned} \right\} \quad \begin{array}{l} \text{body 2} \\ (2.21) \end{array}$$

where  $mR^2_1$  and  $mR^2_2$  are the second moment of inertia about the vertical axis passing through the centre of gravity. The rate of approach and the sliding of the two surfaces at the point of contact can be written as

$$\Delta V_1 = v_1 + v_2 - \dot{\theta}_1 y_1 - \dot{\theta}_2 y_2 \quad (2.22)$$

$$\Delta V_2 = u_1 + u_2 - \dot{\theta}_1 x_1 - \dot{\theta}_2 x_2 \quad (2.23)$$

The addition to these equations is the restitution given by Eq. (2.15) in which when Eq. (2.22) is substituted and then, in the final equation, Eq. (2.20) is substituted, the value of  $F_T$  is evaluated as

$$F_T = \frac{V(1+e)}{C_1 - \lambda C_2} \quad (2.24)$$

where

$$C_1 = \frac{1}{m_1} \left( 1 + \frac{y_1^2}{R^2_1} \right) + \frac{1}{m_2} \left( 1 + \frac{y_2^2}{R^2_2} \right) \quad (2.24a)$$

$$C_2 = \left( \frac{x_1 y_1}{m_1 R^2_1} + \frac{x_2 y_2}{m_2 R^2_2} \right) \quad (2.24b)$$

Using Eqs. (2.20) and (2.21)

$$\begin{aligned} v'_2 &= v'_1 - (F_T/m_1) \\ u'_2 &= u'_1 - (\lambda' F_T/m_1) \end{aligned} \quad (2.25)$$

$$\dot{\theta}_2 = \dot{\theta}_1 + \frac{y_1 - \lambda' x_2}{m_1 R^2_1} F_T$$

$$v''_2 = v''_1 - \frac{F_T}{m_2}$$

$$u''_2 = u''_1 - \frac{\lambda' F_T}{m_2} \quad (2.26)$$

$$\dot{\theta}_2 = \dot{\theta}_1 + \frac{y_2 - \lambda' x_2}{m_2 R_2^2} F_T$$

Figure 2.3 shows plots for Eqs. (2.25) and (2.26). It is interesting to note that larger values of  $\lambda'$  show greater interlocking of the surfaces of the two aircrafts and with  $e$  reaching zero, a greater plastic deformation occurs.

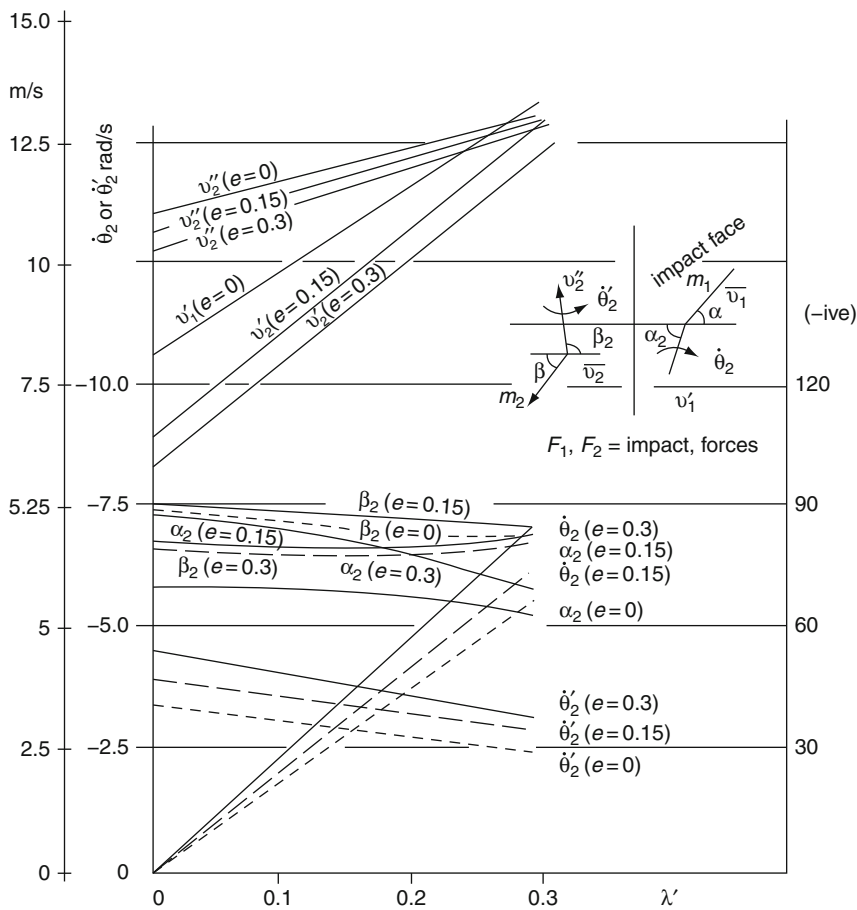


Fig. 2.3 Velocity versus  $\lambda'$  for oblique impact problems

### 2.3.1.4 Case Studies

- (1) One aircraft impacting a rigid barrier, or containment vessel located with no angular velocity

$$\frac{1}{m_2} = 0, \quad v_1 = 0, \quad u_1 = 0, \quad \theta_1 = 0 \quad (2.27)$$

$$C_1 = \frac{1}{m_1} \left( 1 + \frac{y_1^2}{R_1^2} \right); \quad C_2 = \left( \frac{x_1 y_1}{m_1 R_1^2} \right) \quad (2.27a)$$

$$v'_2 = v'_1 (y_1^2 - \lambda' x_1 y_1 - R^2) / \bar{\lambda} \quad (2.27b)$$

$$u'_2 = u'_1 - v'_1 \left( \frac{\lambda' (1 + e) R^2}{\lambda} \right); \quad \dot{\theta}_1 = \frac{(1 + e)(y_1 - \lambda' x_1)}{\lambda} \quad (2.27c)$$

$$\bar{\lambda} = y_1^2 - \lambda' x_1 y_1 + R^2 \quad (2.27d)$$

where

- (2) Circular impactor with radius  $r_1$ .

$$x_1 = r_1 \quad \text{and} \quad y_1 = 0 \quad (2.28)$$

$$v'_2 = e v'_1 \quad (2.28a)$$

$$u'_2 = u_1 - \lambda' v'_1 (1 + e) \quad (2.28b)$$

$$\dot{\theta}_1 = -v'_1 \lambda' r_1 (1 + e) / R^2 \quad (2.28c)$$

For a circular impactor,  $R^2 = 2r_1^2/5$

$$\dot{\theta} = -v'_1 (5\lambda' (1 + e) / 2r_1) \quad (2.28d)$$

- (3) Inelastic collisions. The value of  $e = 0$  in the above case studies:  
Case study (1)

$$\begin{aligned} v'_2 &= v'_1 (y_1^2 - \lambda' x_1 y_1) / \bar{\lambda} \\ u'_2 &= u'_1 - v'_1 (\lambda' R^2 / \bar{\lambda}) \\ \theta_1 &= (y_1 - \lambda' x_1) / \bar{\lambda} \end{aligned} \quad (2.29)$$

Case study (2)

$$\begin{aligned} v'_2 &= 0, \quad u'_2 = u'_1 - \lambda' v'_1 \\ \theta_1 &= -v'_1 \lambda r_1 / R^2 = -2.5 v'_1 \lambda / r_1 \end{aligned} \quad (2.30)$$

(4) Where no interlocking exists,  $\lambda'$  in the above expressions.

This means the aircrafts do not interlock each other but their bodies have created damages.

### 2.3.2 Aircraft Impact on Nuclear Structures – Peak Displacement and Frequency

#### 2.3.2.1 General

A great deal of work has been carried out on the subject of missile and aircraft impact. Tall structures are more vulnerable to civilian, wide-bodied jets or multi-role combat aircraft. A great deal of work on this subject will be reported later. In this section a preliminary analysis is given for the determination of peak displacement and frequency of a tall structure when subject to an aircraft impact. As shown in Fig. 2.4, the overall dimensions of the building are given. Let  $A$  be the base area and  $h$  be the maximum height of the building. According to the principle of the conservation of momentum, if  $m$  is mass and  $v_1$  is the velocity of the aircraft approaching the building, then using a linear deflection profile

$$I(t) = F_1(t) = mv_1 = \left( \frac{\rho Ah}{2g} \right) v_{20} \quad (2.31)$$

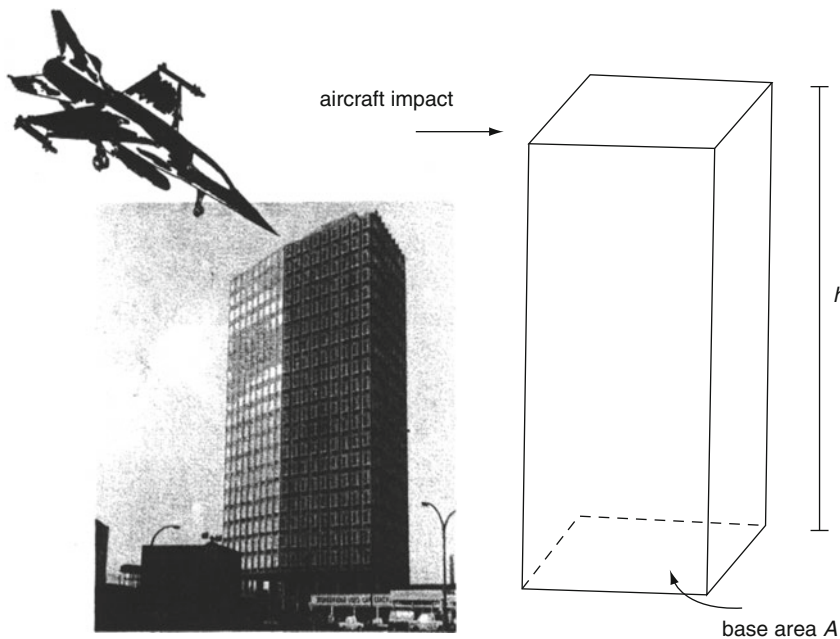


Fig. 2.4

where  $\rho$  is the density or average specific weight and  $v_{20}$  is the velocity of the tip of the nuclear facility.

The initial velocity,  $v_{20}$ , of the facility can thus be evaluated from Eq. (2.31). Free vibrations studied by the time-dependent displacement  $\delta(t)$  is given by

$$\begin{aligned}\delta(t) &= \left(\frac{v_{20}}{\omega}\right) \sin \omega t \\ &= [v_{20}/(2\pi/T)] \sin \omega t \\ &= [v_{20}/\sqrt{(k_s/m_s)}] \sin \omega t\end{aligned}\tag{2.32}$$

where  $\omega$  is the circular frequency and  $k_s$  and  $m_s$  are the equivalent nuclear facility stiffness and mass, respectively.

Using Eq. (2.31) for  $v_{20}$  and  $\sin \omega t = 1$  for  $\delta_{\max}(t)$ , the *peak dynamic displacement*,  $\delta_{\max}(t)$ , is given by

$$\delta_{\max}(t) = mv_1 g T / \pi \rho A h \tag{2.32a}$$

The equivalent point load generated for the peak dynamic displacement is given by Eq. (2.32a). If that load is  $F_1(t)$ , then work done is equal to the energy stored and

$$F_1(t) \times \delta_{\max}(t) = \frac{1}{2} k_s \delta_{\max}^2(t) \tag{2.33}$$

for which

$$F_1(t) = \frac{1}{2} k_s \delta_{\max}(t) \tag{2.33a}$$

While momentum is conserved, a portion of energy of the aircraft is lost on impact. The loss of energy  $E_1$  is then written as

$$E_1 = \frac{1}{3} (\rho A h / m g) (v_{20} / v_1)^2 \tag{2.34}$$

Equation in case study (1) and Eq. (2.29) for inelastic collisions are applied with and without the interlocking parameter,  $\lambda'$ .

The velocity of the new target for the ideal plastic impact is given by

$$\dot{u}_t = [(m_b(t) + m_t)\dot{u}_i^- + m_t\dot{u}_i^-] / [(m_b(t) + 2m_t)] \tag{2.35}$$

Again the superscripts  $+$  and  $-$  indicate just after and just before impact. Wolf et al. (3.169) tested their work on rigid and deformable targets. Data used in their work are reported below:



<div><div>Rigid target</div><div>Boeing 707-320</div><div><math>m_a = 127.5 \text{ Mg}</math></div><div><math>m_w = 38.6 \text{ Mg}</math> included in <math>m_a</math></div><div><math>\epsilon_y = 2 \times 10^{-3}</math>; <math>\epsilon_r = 5 \times 10^{-2}</math></div><div>Deformable target</div><div>Impact area = <math>37.2\text{--}45.1 \text{ m}^2</math></div></div> <div><div>Private Communication Feb 1993.</div><div>Also reported in the Author's book</div><div>"Impact &amp; Explosion 1993" published by</div><div>Blackwell Science, Oxford 1993.</div></div>
---

The tables given for aircrafts and other impacts give data to be used for load–time function or relationship for rigid and deformable targets. The elastic and inelastic systems have been included.

The method of Wolf et al. was idealised into 3D Finite Element method using programs BANG and ISOPAR. Both flexible and rigid targets of 15,000–350,000 isoparametric elements with 750,000 hybrid mixed elements for the aircraft were adopted. The force time–function relationships were combined and they are plotted for various aircrafts. The comparative study is given for these aircraft in (Fig. 2.5). This graph is readily available for the respective impact or crash analysis of any structure. These graphs can be improved by analysing other types of aircrafts.

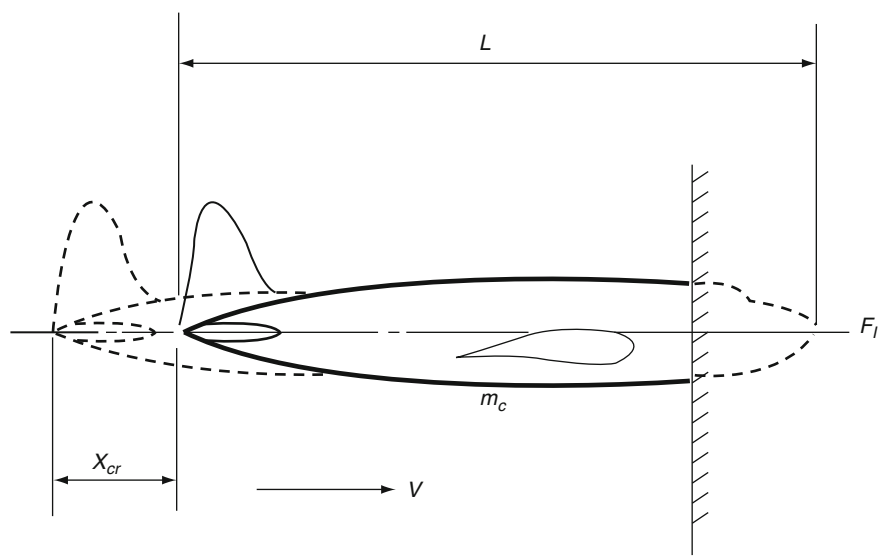


Fig. 2.5 Model aircraft impacting against a rigid surface

2.3.3 Finite Element Applications

This subject has been dealt with in much greater detail in Chapter 3 using dynamic finite element technique. The analysis given under Sections 2.3.1 and 2.3.2 are taken as basis for the finite element approach. Various

load–time functions for different aircrafts have been evaluated so as to suite specific aircraft crash analysis, particularly on containment vessels. A list of containment vessels adopted for various nuclear power stations is given in a tabulated form in Tables 2.24 and 2.25. They can be treated as test examples on the lines given in a sample design example on the TVA containment vessel. The design pressures are given in Tables 2.24 and 2.25 with changed dimensions, loads and material properties; new calculations can be made for the existing vessels and for containments of future BWR and PWR nuclear stations. The dynamic analysis given in chapter 3 can also be used when these containments are accurately analysed under environmental and other anticipated loads such as aircraft and missile crashes, fire and explosion, earthquakes and other hazards.

### 2.3.4 Additional Data on Containment Parameters

#### 2.3.4.1 General Introduction

Tables 2.24 and 2.25 show containments with internal pressures. Some of them are chosen in this section as test examples for readers who wish to test the work in this text.

- (a) *Doel 4*: Status P.W.R 1041 MW in Belgium-FRAMATONE
  - Double walled-double dome resting on piles
  - $R = 21.90$  m inside cylinder
  - Space between walls = 3.34 m
  - Total height = 55 m
  - Spherical domical space = 3.34 m
  - Wall and dome thickness = 0.8–1.3 m
- (b) *Tricastin*: Status P.W.R 900 MW in France-FRAMATONE
  - $R = 18.5$  m inside cylinder
  - Wall thickness = 0.9 m; 12 m buttresses
  - Total height = 59.5 m thick above ground level
  - Base slab = 5 m, base slab = 55.2 m with keys, 1.5 m keys depth variable
- (c) *Civaux*: Status P.W.R 1400 MW in France-FAMATONE
  - Double wall type
  - Double dome type
  - Total height of walls = 545 m
  - Spaces = 3.34 m along the walls
  - Base slab = 50.90 m
- (d) *Sizewell B*: Status P.W.R 1258 MW in UK. WESTING HOUSE
  - Dimensions given as an example in the text

**Table 2.24** Nuclear Power Plants: Containment types and design pressures

Country	Name	Type	Containment type	Design pressure
Argentina	Embalse	PHWR	Steel and RC	
Armenia	Medzamor 2	WER	Reinforced concrete (RC)	0.200
Belgium	Doel 3	PWR	Double PC/RC	0.450
Belgium	Tihange 2	PWR	Double PC/RC	0.450
Belgium	Tihange 3	PWR	Double PC/RC	
Brazil	Angra 1	PWR	Steel and RC	
Bulgaria	Kozloduy 5	WER	Prestressed concrete (PC)	
Canada	Bruce A1	PHWR	Reinforced concrete (RC)	
Canada	Bruce B5	PHWR	Reinforced concrete (RC)	0.291
Canada	Darlington	PHWR	Prestressed concrete (PC)	0.197
Canada	Gentilly 2	PHWR	Prestressed concrete (PC)	0.217
Canada	Pickering B 5	PHWR	Reinforced concrete (RC)	0.141
Canada	Point Lepreau 1	PHWR	Prestressed concrete (PC)	0.104
China	Daya Bay	PWR	Prestressed concrete (PC)	0.520
China	Lingao	PWR	Prestressed concrete (PC)	0.520
China	Qinshan 1	PWR	Prestressed concrete (PC)	0.360
China	Qinshan 3	PHWR	Prestressed concrete (PC)	0.224
China	Qinshan II-1	PWR	Prestressed concrete (PC)	0.450
China	Tianwan	WER	Double PC/RC	0.500
Czech. Rep	Dukovany	WER		
Czech. Rep	Temelin	WER	Prestressed concrete (PC)	0.490
Finland	Olkiluoto (TVO) 1	BWR	Prestressed concrete (PC)	0.470
France	Belleville 1	PWR	Double PC/RC	0.520
France	Blayais 1	PWR	Prestressed concrete (PC)	0.500
France	Bugey	PWR	Prestressed concrete (PC)	0.500
France	Cattenom 1	PWR	Double PC/RC	0.520
France	Chinon B1	PWR	Prestressed concrete (PC)	0.500
France	Chooz 1	PWR	Double PC/RC	0.530
France	Civaux 1	PWR	Double PC/RC	0.530

**Table 2.24** (continued)

Country	Name	Type	Containment type	Design pressure
France	Civaux 2	PWR	Double PC/RC	0.530
France	Cruas 1	PWR	Prestressed concrete (PC)	0.500
France	Dampierre 1	PWR	Prestressed concrete (PC)	0.500
France	Fessenheim	PWR	Prestressed concrete (PC)	0.473
France	Flamanville 1	PWR	Double PC/RC	0.480
France	Golfech 1	PWR	Double PC/RC	0.520
France	Gravelines 1	PWR	Prestressed concrete (PC)	0.500
France	Nogent 1	PWR	Double PC/RC	0.520
France	Paluel 1	PWR	Double PC/RC	0.480
France	Penly 1	PWR	Double PC/RC	0.520
France	St Alban 1	PWR	Double PC/RC	0.480
France	St Laurent B1	PWR	Prestressed concrete (PC)	0.500
France	Tricastin	PWR	Prestressed concrete (PC)	0.500
Germany	Brokdorf	PWR		0.750
Germany	Emsland	PWR	Steel and RC	0.630
Germany	Grafenrheinfeld	PWR		
Germany	Grohnde	PWR		
Germany	Gundremmingen KRB II	BWR	Reinforced concrete (RC)	0.430
Germany	Isar 1	BWR		
Germany	Isar 2	PWR	Steel and RC	0.630
Germany	Krummel	BWR		
Germany	Mulheim Karlich	PWR		
Germany	Neckar 1	PWR	Steel	0.570
Germany	Neckar 2	PWR	Steel and RC	0.630
Germany	Philppsburg 2	PWR		
Germany	Unterweiser	PWR	Steel	0.580
Great Britain	Heysham	AGR	Prestressed concrete (PC)	
Great Britain	Sizewell B	PWR	Double PC/RC	0.445
Great Britain	Tomess PT 1	AGR	Prestressed concrete (PC)	
Hungary	Paks 1	VVER		
India	FBTR Kalpakkam	FR		
India	Kaiga 1	PHWR	Double PC/RC	0.273
India	Kaiga 2	PHWR	Double PC/RC	0.273
India	Kakrapara 1	PHWR	Double PC/RC	0.225
India	Narora 1	PHWR	Double PC/RC	0.225
India	Rajasthan 3	PHWR		0.273

**Table 2.24** (continued)

Country	Name	Type	Containment type	Design pressure
India	Tarapur 3	PHWR	Double PC/RC	0.244
Iran	Bushar	PWR	Steel	
Japan	Fukushima 1-4	BWR	Steel	0.490
Japan	Fukushima 1-6	BWR	Steel	0.385
Japan	Fukushima II-1	BWR	Steel	0.385
Japan	Genkai 4	PWR	Prestressed concrete (PC)	0.500
Japan	Hamaoka 2	BWR	Steel	0.492
Japan	Hamaoka 3	BWR	Steel	0.535
Japan	Ikata 1	PWR	Steel	0.345
Japan	Ikata 3	PWR	Steel	0.389
Japan	Kashiwazaki 4	BWR	Steel	0.416
Japan	Kashiwazaki 6 ABWR	BWR	Reinforced concrete (RC)	0.416
Japan	Kashiwazaki 1	BWR	Steel	0.385
Japan	Mihama 3	PWR	Steel	0.340
Japan	Monju	FR		
Japan	Ohi 1	PWR	Steel	0.540

**Table 2.25** Nuclear Power Plants–PWR, PHWR, RBMK, WER (Containments and design pressures)

Country	Name	Type	Containment type	Design Pressure
Japan	Ohi 3	PWR	Prestressed concrete (PC)	0.500
Japan	Sendai 1	PWR	Steel	0.325
Japan	Shika 1 (NOTO)	BWR	Steel	0.535
Japan	Shimane 2	BWR	Steel	0.535
Japan	Takahama 3	PWR	Steel	0.360
Japan	Tokai 2	BWR	Steel	0.385
Japan	Tomari 1	PWR	Steel	0.360
Japan	Tsuruga 2	PWR	Prestressed concrete (PC)	0.500
Lituania	Ignalina 1	RBMK		
Mexico	Laguna Negra 1	BWR		
Pakistan	Chasma	PWR	Prestressed concrete (PC)	
Romania	Cernavoda	PHWR		
Russia	Balakovo 1	WER	Prestressed concrete (PC)	0.490
Russia	Balakovo 5	WER	Prestressed concrete (PC)	0.490
Russia	Balakovo 6	WER	Prestressed concrete (PC)	0.490
Russia	Kalinin 1	WER	Prestressed concrete (PC)	0.455
Russia	Kalinin 3	WER	Prestressed concrete (PC)	0.490
Russia	Kursk	RBMK		
Russia	Novovoronej 5	WER	Prestressed concrete (PC)	0.455
Russia	Novovoronej 6	WER	Prestressed concrete (PC)	0.490
Russia	Novovoronej7	WER	Prestressed concrete (PC)	0.490

Table 2.25 (continued)

Country	Name	Type	Containment type	Design Pressure
Russia	Rostov 1	WER	Prestressed concrete (PC)	0.490
Russia	Smolensk 1	RBMK		
Slovakia	Bohunice 1	WER		
Slovakia	Mochovce 1	WER		
Slovenia	Krsko	PWR	Steel and RC	
South Africa	Koeberg	PWR	Prestressed concrete (PC)	0.500
South Korea	Kori 3	PWR	Prestressed concrete (PC)	0.520
South Korea	Uljin 1	PWR	Prestressed concrete (PC)	0.500
South Korea	Wolsong 1	PHWR	Prestressed concrete (PC)	0.156
South Korea	Yonggwang 1	PWR	Prestressed concrete (PC)	0.520
Spain	Almaraz 1	PWR		
Spain	Asco 1	PWR	Prestressed concrete (PC)	0.480
Spain	Asco 2	PWR		
Spain	Cofrentes	BWR		
Spain	Trillo 1	PWR		
Spain	Vandellós 2	PWR		
Sweden	Forsmark 3	BWR	Prestressed concrete (PC)	0.600
Sweden	Oskarshamn 3	BWR	Prestressed concrete (PC)	0.600
Sweden	Ringhals 3	PWR	Prestressed concrete (PC)	0.514
Switzerland	Gösgen	PWR	Steel	0.589
Switzerland	Leibstadt	BWR	Steel and RC	0.203
Taiwan	Kuosheng 1	BWR		
Taiwan	Lugmen	ABWR	Reinforced concrete (RC)	
Taiwan	Maanshan 1	PWR		
Ukraine	Khmelnitsky 1	WER	Prestressed concrete (PC)	0.490
Ukraine	Khmelnitsky 2	WER	Prestressed concrete (PC)	0.490
Ukraine	Rovno 1	WER		
Ukraine	Rovno 3	WER	Prestressed concrete (PC)	0.490
Ukraine	Rovno 4	WER	Prestressed concrete (PC)	0.490
Ukraine	Sud Ukraine 1	WER	Prestressed concrete (PC)	0.490
Ukraine	Tchernobyl 3	RBMK		
Ukraine	Zaporozhe 5	WER	Prestressed concrete (PC)	0.490
USA	Braidwood 1	PWR	Prestressed concrete (PC)	0.445
USA	Byron 1	PWR	Prestressed concrete (PC)	0.445
USA	Callaway -1	PWR	Reinforced concrete (RC)	
USA	Catawba 1	PWR	Steel and RC	0.204
USA	Clinton 1	BWR	Reinforced concrete (RC)	0.204
USA	Comanche 1	PWR	Reinforced concrete (RC)	0.445

**Table 2.25** (continued)

Country	Name	Type	Containment type	Design Pressure
USA	Gran Gulf 1	BWR	Reinforced concrete (RC)	0.203
USA	Hatch 2	BWR		
USA	Hope Creek	BWR	Steel	0.528
USA	La Salle 1	BWR	Prestressed concrete (PC)	0.410
USA	Millstone 3	PWR	Reinforced concrete (RC)	
USA	Nine Mile Point 2	BWR	Reinforced concrete (RC)	0.411
USA	Palo Verde 1	PWR	Prestressed Concrete (PC)	0.514
USA	Perry 1	BWR	Steel	0.204
USA	River Bend 1	BWR	Steel	0.204
USA	San Onofre 2	PWR	Prestressed concrete (PC)	0.514
USA	Seabrook 1	PWR	Reinforced concrete (RC)	0.459
USA	Shearon-Harris 1	PWR	Reinforced concrete (RC)	
USA	Shoreham	BWR	Reinforced concrete (RC)	0.389
USA	South Texas	PWR	Prestressed concrete (PC)	
USA	St. Lucie 2	PWR	Steel and RC	0.376
USA	Summer 1	PWR	Prestressed concrete (PC)	
USA	Susquehanna 1	BWR	Reinforced concrete (RC)	
USA	Vogtle 1	PWR	Prestressed concrete (PC)	0.459
USA	Waterford 3	PWR	Steel and RC	
USA	Watts Bar 1	PWR	Steel and RC	0.193
USA	WNP-2 Hanford	BWR	Steel	
USA	Wolf Creek	PWR	Prestressed concrete (PC)	

(e) *GenKai 4*: P.W.R 1180 MW in Japan-MITSUBISHI $R = 22.150$  m

Total height of walls = single-type 43 m wall thickness = 0.75–1.3 m

Single dome height = 22.6 m

Dome thickness = 1 m

Dome radius = 22.650

Base slab inclusive galleys = 44.30 m

Thickness varies from 10.2 m to 15.8 m

(f) *Kaiga-I*: P.H.W.R 220 MW in India (Double Wall Type) $R =$  radius inside = 21.28 m

Total height of the wall = 48.235 m

Inner space of walls = 2.0 m

Inner space of dome = 2.0 m  
 Radius to centroid = 33.57 m inner  
 Radius of the dome spherical = 39.60 outer  
 Base slab (without keys) thickness = 3.5 m  
 Base slab (with keys) thickness = 5.5 m  
 Base slab total dimension = 49.0 m  
 Key base = 8.5 m

*Note:* LOCA ranges in all from 0.3 to 0.35 MPa. Exceptional causes LOCA = 0.47–0.60 MPa related to BWR types.

## References

1. ANSI A58.1-1972. Building Code Requirements for Minimum Design Loads in Buildings and Other Structures. American National Standards Institute, 1972.
2. Shah, H. C. et al. A Study of Seismic Risk for Nicaragua, Part 1, The J. A. Blume Earthquake Engineering Center, Report No. 11, Dept. of Civil Engineering, Stanford University, 1975.
3. Wiggins, J. H. Procedure of Determining Acceptable Risk Ground Motion Design Criteria. Technical Report No. 75-1229, J. H. Wiggins Company, Redondo Beach, CA, 1975.
4. Der Kureghian, A. and Ang, A. H-S. A Line Source Model for Seismic Risk Analysis, Structural Research Series No. 419, University of Illinois at Urbana-Champaign, Urbana, IL, October 1975.
5. Specification for the Design, Fabrication and Erection of Structural Steel for Buildings. American Institute of Steel Construction, 1969.
6. Uniform Building Code, 1976 edn, Vol. 1, International Conference of Building Officials, 1976.
7. ACI Standard Building Code Requirements for Reinforced Concrete (ACI-318-71). American Concrete Institute, 1970.
8. ASME Boiler and Pressure Vessel Code Section III, Division I. Rules for Construction of Nuclear Power Plant Components. American Society of Mechanical Engineers, 1974.
9. ACI-ASME Joint Technical Committee. Code for Concrete Reactor Vessels and Containments. ASME Boiler and Pressure Vessel Code Section III, Division 2 and ACI Standard 359-74, 1975.
10. ACI Standard Code Requirements for Nuclear Safety Related Concrete Structures (ACI-349.7R). American Concrete Institute, 1975.
11. Specification for Steel Railway Bridges, Cooper E-72 Loading. American Railway Engineering Association, 1972.
12. Standard Specification for Highway Bridges, HS20-S16 Loading. American Association of State Highway Officials.
13. Federal Regulation 10 CFR Part 100, Reactor Site Criteria, Appendix A. Seismic and Geological Siting Criteria for Nuclear Power Plants. November 1973.
14. Tong, W. H. Seismic Risk Analysis for Two-Sites Case. Publication No. R75-22, Department of Civil Engineering, M.I.T., May 1975.
15. ANSI A58.1-1972, Building Code Requirements for Minimum Design Loads in Buildings and Other Structures, American National Standards Institute.
16. Newmark, N. M. Overview of Seismic Design Margins. Paper presented at A.I.F. Workshop on Reactor Licensing and Safety, December. 1974.



17. Hsieh, T., Okrent, D., and Apostolakis, O. E. On the Average Probability Distribution of Peak Ground Acceleration in the U.S. Continent Due to Strong Earthquakes. UCLA-ENG-75 16, University of California at Los Angeles, March 1976.
18. Anderson, D. L., Chariwood, R. G., and Chapman, C. B. On seismic risk analysis of nuclear plants safety systems, *Canadian Journal of Civil Engineering*, Vol. 2, No. 4, 1975, pp. 558–571.
19. St. Amand, P. Two proposed measures of seismicity, *Bulletin of the Seismological Society of America*, Vol. 46, 1961.
20. Howell, B. F., Jr., et al. Integrated and frequency band magnitude, two alternative measures of the size of an earthquake, *Bulletin of the Seismological Society of America*, Vol. 60, No. 3, 1970.
21. Blume, J. A. An engineering intensity scale, *Bulletin of the Seismological Society of America*, Vol. 60, No. 1, 1970.
22. Blume, J. A. and Monroe, R. E. The Special Matrix Method of Predicting Damage from Ground Motion, John A. Blume & Associates, Research Division, San Francisco, CA, for Nevada Operations Office, U.S. Atomic Energy Commission, 1971.
23. Trifunac, M. D. and Brady, A. G. On the correlation of seismic intensity scales with the peaks of recorded strong ground motion, *Bulletin of the Seismological Society of America*, Vol. 65, No. 1, 1975, pp. 139–162.
24. Richter, C. F. An instrumental earthquake scale, *Bulletin of the Seismological Society of America*, Vol. 25, 1935.
25. Aki, K. Generation and Propagation of G Waves from Niigata Earthquake of June 16, 1964, part 2, Estimation of Earthquake Moment, Released Energy and Stress-Strain Drop from G-Wave Spectrum, *Bulletin of the Earthquake Research Institute, Tokyo University*, Vol. 44, 1966 pp. 73–88.
26. Cornell, C. A. and Vanmarcke, E. H. The major influences on seismic risk. *Proceedings of the 4th World Conference on Earthquake Engineering*, Santiago, Chile, 1969.
27. Algermissen, S. I. Seismic risk studies in the United States. *Proceedings of the 4th World Conference on Earthquake Engineering*, Vol. 1, Santiago, Chile, 1969.
28. Algermissen, S. T. and Perkins, D. M. Earthquake risk studies in the branch of seismicity and risk analysis. Presented at USGS Earthquake Studies Advisory Panel, Colorado School of Mines, Golden, CO, June 4–5, 1975.
29. Liu, S. C. and Fagel, L. W. Seismic risk analysis—comparison of three different methods. for seismic regionalization, *Bulletin of the Seismological Society of America*, Vol. 65, No. 4, 1975, pp. 1023–1027.
30. Esteva, L. Seismic prediction, a bayesian approach. *Proceedings of the 4th World Conference on Earthquake Engineering*, Vol. 1, Santiago, Chile, 1969.
31. Mortgat, C. P. Bayesian Approach to Seismic Hazard Mapping. Ph.D. Thesis, Stanford University, 1976.
32. Esteva, L. Regionalization Seismica de Mexico para fines de Ingenieria. Report 246, Institute of Engineering, National University of Mexico, Mexico City, 1970.
33. Esteva, L. Seismic risk and seismic design input for nuclear power plants. *Seismic Design for Nuclear Power Plants*, ed. R.J. Hansen, MIT Press, Cambridge, MA, 1970, pp. 438–483.
34. Cloud, W. K. and Perez, V. Unusual accelerograms recorded at Lima, Peru, *Bulletin of the Seismological Society of America*, Vol. 61, 1970, pp. 663–640.
35. Schnabel, P. and Seed, H. B. Accelerations in rock for earthquakes in the western United States, *Bulletin Seismological Society America*, Vol. 63, 1973, pp. 501–516.
36. Gupta, I. N. and Nuttli, O. W. Spatial attenuation of intensities for central U.S. earthquakes, *Bulletin Seismological Society America*, Vol. 66, No. 3, 1976, pp. 743–751.
37. Seed, H. B., Murarka, R., Lysmer, J., and Idriss, I. M. Relationships of maximum acceleration, maximum velocity, distance from source and local site conditions for moderately strong earthquakes, *Bulletin Seismological Society America*, Vol. 66, No. 4, 1976, pp. 1323–1342.

38. Cough, R. W. Earthquake analysis by response spectrum superposition, *Bulletin Seismological Society America*, Vol. 52, No. 3, 1962.
39. Blume, J. A., Sharpe, R. L., and Dalal, J. S. Recommendations for Shape of Earthquake Response Spectra. John A. Blume and Associates, Engineers, San Francisco, CA, February 1973 (USAEC Report No. WASH-1254).
40. Mohraz, B., Hall, W. J., and Newmark, N. M. A Study of Vertical and Horizontal Earthquake Spectra. Nathan N. Newmark Consulting Engineering Services, Urbana, IL, 1972 (USAEC Report No. WASH-1255).
41. Seed, H. B., Ugas, C., and Lysmer, J. Site Dependent Spectra for Earthquake Resistant Design, Report No. EERC-74-12, U.C. Berkeley, 1974.
42. McGuire, R. K. Seismic Design Spectra and Mapping Procedures Using Risk Analysis Based Directly on Oscillator Response. Branch of Seismicity and Risk Analysis, USGS, Denver, CO, 1975.
43. Trifunac, M. D. Preliminary empirical model for scaling Fourier amplitude spectra of strong ground acceleration in terms of earthquake magnitude, source-to-station distance, and recording site conditions, *Bulletin Seismological Society America*, Vol. 66, No. 4, 1976, pp. 1343–1373.
44. Dobry, R. et al. Influence of magnitude, site conditions and distance on significant duration of earthquakes. The 6th World Conference on Earthquake Engineering, New Delhi, India, January 1977.
45. Bolt, B. A. Duration of strong motion. Proceedings of the 5th World Conference on Earthquake Engineering, Paper 292, Rome, 1973.
46. NRC Standard Review Plan Section 2.5.2.11.3, Vibratory Ground Motion Acceptance Criteria, U.S. Nuclear Regulatory Commission, Office of Nuclear Reactor Regulation, June 1975.
47. Shakal, A. F. and Toksoz, M. N. Earthquake hazard in New England, *Science*, Vol. 195, 1977, pp. 171–173.
48. Thom, H. C. S. New distributions of extreme winds in the United States, *Journal of the Structural Division, ASCE*, Vol. 94, No. ST7, Proc. Paper 6038, 1968, pp. 1787–1801.
49. Simiu, E. Probabilistic models of extreme wind speeds: uncertainties and limitation. Proceedings of the 4th International Conference on Wind Effect on Structures and Buildings, London, England, September 1975, pp. 53–62.
50. Russell, L. R. Probability distributions for hurricane effects, *Journal of Waterways, Harbors and Coastal Engineering Division, ASCE*, Vol. 97, No. WW 1, 1971, pp. 139–154.
51. Tryggvason, B. V., Surry, D., and Davenport, A. G. Predicting wind-induced response in hurricane zones, *Journal of the Structural Division, ASCE*, Vol. 102, No. ST12, 1976, pp. 2333–2351.
52. Sklarin, J. Probabilities of Hurricanes. Dept. of Civil Engineering, Research Report, MIT, Cambridge, MA, February 1977.
53. Fujita, T. T. Estimates of Areal Probability of Tornadoes from Inflationary Reporting of their Frequencies. Satellite and Mesometeorology Research Project (University of Chicago), SMRP Research Paper No. 89, October 1970.
54. Thom, H. C. S. Tornado probabilities, *Monthly Weather Review*, Oct–Dec 1963, pp. 730–736.
55. Pautz, M. E. (ed.). Severe Local Storm Occurrences, 1955–1967, U.S. Department of Commerce, Environmental Science Services Administration, ESSA Tech. Memo. VBTM FCST 12, September 1969.
56. USNRC, Regulatory Guide 1.76, Design Basis Tornado for Nuclear Power Plants, Directorate of Regulatory Standards, April 1974.
57. Garson, R. C., Catalan, J. M., and Cornell, C. A. Tornado design winds based on risk, *Journal of the Structural Division, ASCE*, Vol. 101, No. ST9, 1975, pp. 1883–1897.
58. Hoecker, W. H., Jr. Wind speed and air flow patterns in the Dallas tornado of April 2, 1957, *Monthly Weather Review*, Vol. 88, No. 5, 1960, pp. 167–180.

59. Hoecker, W. H., Jr. Three dimensional pressure patterns of the Dallas tornado and some resultant implications, *Monthly Weather Review*, Vol. 89, No. 12, 1961, pp. 533–542.
60. Wen, Y. K. and Ang, A. H-S. Tornado risk and wind effect on structures. *Proceedings of the 4th International Conference on Wind Effect on Buildings and Structures*, London, England, September 1975, pp. 63–73.
61. Wen, Y. K. Note on analytical modeling in assessment of tornado risks. *Proceedings of Symposium on Tornadoes, Assessment of Knowledge and Implications for Man*, June 1976, Texas Tech University, Lubbock, TX.
62. Wen, Y. K. Dynamic wind loads on tall buildings, *Journal of the Structural Division*, ASCE, Vol. 101, No. ST1, 1975, pp. 169–185.
63. Kuo, H. L. Axisymmetric flow in the boundary layer of a maintained vortex, *Journal of Atmospheric Sciences*, Vol. 28, No. 1. 1971, pp. 20–41.
64. McDonald, J. R., Minor, J. E., and Mehta, K. C. Tornado generated missiles. *Specialty Conference on Structural Design of Nuclear Power Plant Facilities*, Chicago, IL, December 17–18, 1973, *Proceedings (Publ.: ASCE)*, Vol. II, pp. 543–556.
65. McDonald et al. Tornado generated missiles. *Int. Conf. Nuclear Plant Facilities*, Dec. 1973 ASCE, Vol. 11, pp. 543–556.
66. Abbey, R. F. and Fujita, T. T. Use of tornado path length and gradations of damage to assess tornado intensity probability. *proceedings of the 9th Conference on Severe Local Storms*, Norman, Oklahoma, 1975.
67. Abbey, R. F. Risk probabilities associated with tornado windspeeds. *Proceedings of the Symposium on Tornadoes, Assessment of Knowledge and Implication for Man*, June 1976. Texas Tech University, Lubbock, TX.
68. American Nuclear Society, ANS 24, Draft American National Standard, Tsunami Guidelines at Power Reactor Sites, ANSI N515, December 1975.
69. Wiegel, R. L. *Earthquake Engineering*. Prentice-Hall, Englewood Cliffs, NJ, 1970.
70. Gumbel, E. J. *Statistical Theory of Extreme Values and Some Practical Applications*, National Bureau of Standards, Applied Mathematics Series, No. 33, Superintendent of Documents, U.S. Government Printing Office, Washington, 1954.
71. Gumbel, E. J. *Statistics of Extremes*. Columbia University Press, New York, NY, 1958.
72. Wall, I. B. Probabilistic assessment of flooding hazard for nuclear power plants, *Transactions of the American Nuclear Society*, Vol.16, No.211, 1973; *Nuclear Safety*, Vol. 15, No. 4, 1974, pp. 399–408.
73. Linsley, R. K., Kohler, M. A., and Pauthus, J. L. H. *Hydrology for Engineers*, 2nd edn. McGraw-Hill, New York, NY, 1975.
74. Shane, R. M. and Lynn, W. R. Mathematical model for flood risk evaluation, *Journal of the Hydraulics Division*, ASCE, Vol. 90, No. HY6, 1964, pp. 1–20.
75. Linsley, R. K. and Franzini, J. B. *Water Resources Engineering*, 2nd edn. McGraw-Hill, New York, NY, 1972.
76. Linsley, R. K., Kohler, M., and Paulhus, J. L. H. *Applied Hydrology*. McGraw-Hill, New York, NY, 1949.
77. U.S. Weather Bureau. *Rainfall Frequency Atlas of the United States for Durations from 30 Minutes to 24 Hours and Return Period from 1 to 100 Years*, Weather Bureau Technical Paper No. 40, Washington, D.C., 1964.
78. U.S. Weather Bureau. *Seasonal Variation of the Probable Maximum Precipitation East of the 105th Meridian for Areas from 10 to 1000 Square Miles and Durations of 6, 12, 24 and 48 Hours*, Hydrometeorological Report No. 33, U.S. Weather Bureau, 1956.
79. Browzin, B. S. Statistical safety factor concept for determining the probable maximum flood. *Specialty Conference on Structural Design of Nuclear Power Plant Facilities*, Chicago, IL, December 1973; *Proceedings (Publ. ASCE)*, Vol. II, pp. 557–570.
80. USNRC Standard Review Plan, Section 2.4.3, Probable Maximum Flood (PMF) on Streams and Rivers, U.S. Nuclear Regulatory Commission, Office of Nuclear Reactor Regulation, September 1975.

81. American Nuclear Society. Draft American National Standard, Guidelines for Determining Design Basis Flooding at Power Reactor Sites, ANSI N 170.
82. USNRC Standard Review Plan, Section 3.5.1, U.S. Nuclear Regulatory Commission, Office of Nuclear Reactor Regulation, September 1975.
83. Electric Power Research Institute. Tornado Missile Risk Analysis, EPRI NP- 154, Project 616-I, Topical Report 1, January 1975.
84. Johnson, B. Tornado Missile Risk Analysis, Study Being Conducted for Boston Edison Power Company by Science Applications, Inc., Private Communication, 1976.
85. Bush, S. H. Probability of damage to nuclear components due to Turbine Failure, U.S.A.E. C., ACRS, and Pacific Northwest Laboratories, Battelle Memorial Institute, November 6, 1972.
86. Bush, S. H. Probability of damage to nuclear components due to turbine failure, Nuclear Safety, Vol. 14, No. 3, 1973, pp. 187–201.
87. Emmert, H. D. Investigation of large steam-turbine spindle failure, Mechanical Engineering, Mechanical Engineering, 1956, p. 46.
88. Rankin, A. W. and Seguin, B. R. Report of the investigation of the turbine-wheel fracture at Tanners Creek, Mechanical Engineering, 1956, p. 47.
89. Schabtach, C., Fogleman, E. L., Rankin, A. W., and Winne, D. H. Report of the investigation of two generator-rotor fractures, Mechanical Engineering, p. 48, 1956.
90. Peterson, R. E., Mochel, N. L., Conrad, J. D., and Gunther, D. W. Large rotor forgings for turbines and generators, Mechanical Engineering, p. 49, 1956.
91. Lindley, A. L. G. and Brown, F. H. S. Failure of a 60-MW steam turbo-generator at Uskmouth Power Station, Proceedings of the Institution of Mechanical Engineers, Vol. 172, 1958, p. 627.
92. Kalderon, D. Steam turbine failure at Hinkley Point 'A', Proceedings of the Institution of Mechanical Engineers, Vol. 186, 1972, p. 341. Hinkley Point 'A' Power Station, Proceedings of the Institution of Mechanical Engineers, Vol. 186, 1958, p. 379.
93. Codier, E. O. Reliability growth in real life. Proceedings of the IEEE Annual Symposium on Reliability, Boston, January 1968;— Duane, J. T. General Electric Company Report DF62 MD300.
94. Downs, J. E. Hypothetical Turbine Missiles—Probability of Occurrence, General Electric Co., Turbine Dept., Memo Report, March 1973.
95. Analysis of the Probability of the Generation and Strike of Missiles from a Nuclear Turbine, Westinghouse Electric Corp., Steam Turbine Division Engineering, March 1974.
96. Hagg, A. C. and Sankey, G. O. The containment of disk burst fragments by cylindrical shells, Transactions of the ASME, Journal of Engineering for Power, Vol. 96, 1974, pp. 114–123.
97. Report Covering the Effects of a Turbine Accelerating to Destructive Overspeed, Westinghouse Electric Corp., Report 196/381 A, 1974.
98. Report Covering the Effects of a High Pressure Turbine Rotor Fracture and Low Pressure Turbine Disc Fractures at Design Overspeed, Westinghouse Electric Corp., Report 196/381 B, 1974.
99. Turbine Missile Analysis, Allis-Chalmers Power Systems Inc., Report Contained in Grand Gulf PSAR (Docket No. 50-416), Amendment 6, April 1973.
100. Downs, J. E. Hypothetical Turbine Missile Data, 43-Inch Last Stage Bucket Units, General Electric Co., Turbine Dept., Memo Report, March 1973.
101. Semanderes, S. N. Methods of Determining the Probability of a Turbine Missile Hitting a Particular Plant Region, WCAP-786I, Westinghouse Electric Corp., 1972.
102. Semanderes, S. N. Method of determining missile impact probability, Transactions of the American Nuclear Society, Vol. 15, No. 1, 1972, p. 401.
103. O'Connell, W. J., Bascheire, R. J. Design applications of turbine missile impact Analysis. Proceedings of the 2nd ASCE Specialty Conference on Structural Design of Nuclear Plant Facilities, New Orleans, LA, December 1975 (publ. ASCE), pp. 541–561.

104. O'Connell, W. J. and Fortney, R. A. Turbine missile impact analysis: a detailed treatment, Transactions of the American Nuclear Society, Vol. 19, 1974, p. 231; EDS Nuclear Inc., Report, October 27, 1974.
105. Swan, S. W. and Meleis, M. A method of calculating turbine missile strike and damage probabilities, Nuclear Safety, Vol. 16, 1975, pp. 443–451.
106. Bhattacharya, A. K. and Chaudhuri, S. K. The Probability of a turbine missile hitting a particular region of a nuclear power plant, Nuclear Technology, Vol. 28, 1976, pp. 194–198.
107. Johnson, B. et al. Analysis of the Turbine Missile Hazard to the Nuclear Thermal Power Plant at Pebble Springs, Oregon, Science Applications Inc. Report to the Portland General Electric Company, PGE-2012, January 1976.
108. Hornyik, K. Hazards to nuclear plants from surface traffic accidents, Nuclear Technology, Vol. 25, 1975, pp. 651–657.
109. USNRC Standard Review Plan, Section 3.5.1.6, Aircraft Hazards, U.S. Nuclear Regulatory Commission, Office of Nuclear Reactor Regulation, September 1975.
110. Census of U.S. Civil Aircraft, Office of Management Systems, Federal Aviation Administration, Department of Transportation.
111. Analysis of Aircraft Accident Data, U.S. Civil Aviation, National Transportation Safety Board, Department of Transportation.
112. Chelapati, C. V., Kennedy, R. P., and Wall, I. B. Probabilistic assessment of aircraft hazard for nuclear power plants, Nuclear Engineering and Design, Vol. 19, 1972, pp. 333–364.
113. Wall, I. B. and Augensteiff, R. C. Probabilistic assessment of aircraft hazard to a nuclear power plant – I, Transactions of the American Nuclear Society, Vol. 13, 1970, p. 217.
114. Chelapati, C. V. and Wall, I. B. Probabilistic assessment of aircraft hazard for nuclear power plants – II, Transactions of the American Nuclear Society, Vol. 13, 1970, p. 218.
115. Wall, I. B. Probabilistic assessment of aircraft risk for nuclear power plants, Nuclear Safety, Vol. 15, No. 3, 1974.
116. Long Island Lighting Co., Shoreham Station (Docket 50-322), Amendment No. 3, February 1969.
117. Solomon, K. A. Hazards associated with aircrafts and missiles, Transactions of the American Nuclear Society, Vol. 23, 1976, p. 312.
118. Hornyik, K. Airplane crash probability near a flight target, Transactions of the American Nuclear Society, Vol. 16, 1973, p. 209.
119. Hornyik, K. and Grund, J. E. Evaluation of air traffic hazards at nuclear power plants, Nuclear Technology, Vol. 23, 1974, pp. 28–37.
120. NRC Regulatory Guide 1.70, Standard Format and Content of Safety Analysis Reports for Nuclear Power Plants, LWR Edition, Revision 3, NUREG-75/094, U.S. Nuclear Regulatory Commission, Office of Standards Development, September 1975.
121. Aircraft crash probabilities, Nuclear Safety, Vol. 17, 1976, pp. 312–314.
122. Hahn, G. J. and Shapiro, S. S. Statistical Models in Engineering. Wiley, New York, NY, 1967.
123. Julian, O. G. Synopsis of first progress report of committee on safety factors, Journal of the Structural Division, Proceedings of the ASCE, Vol. 83, No. ST4, 1957.
124. Kececioglu, D. Reliability analysis of mechanical components and systems, Nuclear Engineering and Design, Vol. 19, 1972, pp. 259–290.
125. Report of ASCE-ACI Joint Committee on Ultimate Strength Design, Proc. Sep. No. 809, ASCE, Vol. 81, October 1955.
126. Sexsmith, R. O. Reliability Analysis of Concrete Structures, Technical Report No. 83, Dept. of Civil Engineering, Stanford University, Stanford, CA, August 1967.
127. Andersen, P. The Resistance to Combined Flexure and Compression of Square Concrete Members, University of Minnesota Engineering Experiment Station Technical Paper No. 29, University of Minnesota, 1941.

128. Veist, E. and Hognestad, E. Sustained load strength of eccentrically loaded short reinforced concrete columns, *ACI Proceedings*, Vol. 52, 1956, pp. 727–755.
129. Chelapati, C. V. and Wall, I. B. Probabilistic assessment of seismic risk for nuclear power plants, *Transactions of the American Nuclear Society*, Vol. 12, 1969, p. 684; Holmes and Narver, Inc. Report, December 1969.
130. Hadjian, A. H. and Hamilton, C. W. Probabilistic frequency variations of concrete structures. 2nd International Conference on Structural Mechanics in Reactor Technology, Berlin, 1973; Paper K-3/5.
131. Stevenson, J. D. and Moses, F. Reliability analysis of framed structures, *Journal of the Structural Division, ASCE*, Vol. 96, No. ST1 1, Proc. Paper 7692, 1970.
132. Riera, J. O. On the stress analysis of structures subjected to aircraft forces. *Nuclear Engineering and Design*. North Holland Publishing, Amsterdam, Holland, 1968, p. 8.
133. Long Island Lighting Co., Shoreham Station (Docket 50-322), Amendment No. 3, February 1969.
134. United Engineers and Constructors, Seabrook Station Containment Aircraft Impact Analysis, Prepared for Public Service Co. of New Hampshire, Seabrook, New Hampshire, Revision 1, January 1975.
135. NRC Standard Review Plan Section 3.6.1, Plant Design for Protecting Against Postulated Piping Failures in Fluid Systems Outside Containment, U.S. Nuclear Regulatory Commission, Office of Nuclear Reactor Regulation, March 1975.
136. NRC Standard Review Plan Section 3.6.2, Determination of Break Locations and Dynamic Effects Associated with Postulated Rupture of Piping, U.S. Nuclear Regulatory Commission, Office of Nuclear Reactor Regulations, March 1975.
137. ANS 58.2 Committee, Design Basis for Protection of Nuclear Power Plants Against Effects of Postulated Rupture,” ANS-N 176, January 1977 (Draft).
138. Marcal, P. V. Finite element analysis with material Nonlinearities theory and practice. *Pressure Vessel and Piping Design and Analysis*, Vol. 1. American Society of Mechanical Engineers, 1972, p. 486.
139. AEC Standard Review Plan Section 3.8.1, Concrete Containment, U.S. Atomic Energy Commission, Directorate of Licensing, 1974.
140. AEC Standard Review Plan Section 3.8.3, Concrete and Steel Internal Structure of Steel and Concrete Containments, U.S. Atomic Energy Commission, Directorate of Licensing, 1974.
141. ASME code Section 3 Division 2. ACI code for PCCV and PCRV, Article CC 6000, 1989.
142. Axcell, Containment cooling by water film, *The Nuclear Engineer*, Vol. 42, Number 1, 2001.
143. Basu, K. Containment construction using HPC (i\EB) India. *Proceedings of seminar on containments of nuclear reactors in conjunction with 15th SMIRT*, Seoul, 1999.
144. Chataigner, Granger, Touret et al. Containment leakage under accident conditions. *Proceedings of Seminar on Containment of Nuclear Reactors in Conjunction with 15th SMIRT*, Seoul, 1999.
145. Costaz. Le béton hautes performances (HPC), RGN No 4, 1992.
146. Costaz (EDF Septen), 15–22 November, Infrastructures for energy, Keynote, IFTA Seminar on Civil Engineering and Architecture, 1992.
147. Costaz, Picaut, Chataigner. Delayed Phenomena Analysis from French PWR 900 MW containment. Monitoring comparison with foreseen design values. *SMIRT 10*, 1989.
148. Danish, Hansen, Liersch, Peter. Testing of a concrete containment model coated with a composite liner. *SMIRT 14*, Vol. 5 Div. H concrete structures. HW/2, 1997.
149. Danisch, Hansen. Status report on German containment composite liner research. *Proceedings of Seminar on Containment of Nuclear Reactor in Conjunction with 15th SMIRT*, Seoul, 1999.
150. De Larrare, Ithualde, Acker, Chauvel. HPC for NPP, 2nd International Conference on Utilisation of HSC, Berkeley, ACISP, 1990.



151. FIP – Fédération Internationale de la Précontrainte, state-of-art report: Design and construction of prestressed concrete reactor vessels, June 1978.
152. Granger, Labbé. Mechanical and leak tightness behaviour of a containment mock-up under severe accident – SMIRT 14, Vol. 5 Div. H concrete structures. HW/1, 1997.
153. Guinet, Decelle, Lancia, Barré. Design and erection of a large mock-up of containment under severe accident conditions – SMIRT 14, Vol. 5 Div. H concrete structures. HW/3, 1997.
154. Hessheimer, Pace, Klamerus, Matsumoto, Costello Instrumentation and testing of a PCCV model –. SMIRT 14, Vol. 5 Div. H concrete structures. H03/4, 1997.
155. IAEA – TECDOC-1025. Assessment and management of ageing of major nuclear power plant components important to safety: concrete containment buildings, June 1998.
156. Irving, Hinley, and Palfrey. The design, analysis and testing of the 1/10 scale model of the sizewell B containment building. International Conference on Structural Design For Hazardous Loads, Institution of Structural Engineers, Brighton, UK, 17–19 April 1991.
157. Jolivet, Richli, A seismic foundation system for nuclear power stations, SMIRT 4, Vol. K (b), 1977.
158. Kikuchi, Kobanashi, Ichizono. SIT, Kashiwazahi Kariwa, RCCV. Structural Integrity test of reinforced concrete containment at Kashiwazaki-Kariwa. SMIRT 14. Vol. 5 Div. H concrete structures. H03/5 - H03/6, 1997.
159. Klymov (State Research Institute of Building Construction, Kiev). Monitoring of stressed-strained state and forces in cables of prestressed containment shells of NPPs. Joint Wano/OECD-NEA. Workshop, Civaux, Poitiers, France, 1997.
160. Klymov (State Research Institute of Building Construction). Results and Problems of Monitoring of Prestressed Containment of Nuclear Power Plants. OECD-NEA. Workshop, Tractebel-Brussels, Belgium, 2000.
161. Kuroda et al. Recent advances in concrete containment vessels in Japan, Nuclear Engineering and Design, Vol. 140, 1993.
162. Kuroda, Hasegawa. Recent topics on concrete containment vessels in Japan: verification of SIT and assurance of safety margins, Japan. Proceedings of Seminar on Containment of Nuclear Reactors in conjunction with 5th SMIRT, Seoul, 1999.
163. Libmann. Elements de Sûreté Nucléaire – IPSN. Published by Lavoisier, France, 1997.
164. Maliavine Atom Energoproject Russian Federation. Prestress losses in containments of VVER 1000 Units. Joint Wano/OECD-NEA. Workshop, Civaux, Poitiers, France, 1997.
165. McFarlane, Smith, Davies, Millustry. In-service monitoring of AGR and PWR Nuclear Safety related Structures in the UK, Institution of Nuclear Engineers, September 1996, Cambridge, UK.
166. McFarlane, Smith. Plant Life Management. European Commission, Directorate General, FISA 99 Symposium, Luxembourg, 1999.
167. Martinet, Guinet, Roussel, Granger. Prestress losses in NPP containments: the EDF experience. Joint Wano/OECD-NEA. Workshop, Civaux, Poitiers, France, 1997.
168. OECD-NEA Nuclear Regulation. Regulatory aspects of life extension and upgrading of MPPs. CNRA Special Issues, Meeting 2000 Report, January 2001.
169. Picaut, Sidaner, Pastor, Lorteau. The dome of Daya Bay containment, design and construction, SMIRT 11, 1991.
170. Proceedings of seminar on containment of Nuclear Reactor in Conjunction with 15th SMIRT, Seoul. Thomas Jueger Seminar, 1999.
171. RCCG, Design and construction rules for civil works of PWR Nuclear Islands.
172. Roy, Guinet, Barré. Concrete monitoring analysis during the prestressing of a containment and comparison with foreseen design values – SMIRT 14. Vol. 5 Div. H concrete structures, HO 1/2, 1997.
173. Saito, H. et al. Experimental study on RCCV of ABWR plant. SMIRT 10, 1989.

174. Setogawa, Sakarai, Funokoshi, Yemaguchi, Koike, Kamei, and Hagro. Structural Integrity tests of prestressed concrete containment vessels at Ohi NPP, SMIRT 12, Vol H, 1993.
175. SFEN, Proceedings of International Conference on the EPR Project SMIRT 14, August 97, Vol. 5, Div. H concrete structures. H 04/3 PSA of typical 900 MW French nuclear containment. Grangier, Chataigner, November 1995.
176. Smith, L.M. and Taylor, M.F. The Long term In-Service Performance of Corrosion Protection to Prestressing Tendons in AGR PCPVS, Joint Wano/OECD-NEA Workshop, Civaux, Poitiers, France, 1997.
177. Smith, De Marneffe, Mathet, Contri. Civil Engineering Instrumentation on Nuclear Power Plants – An International Perspective, Institution of Nuclear Engineers, November 2000.
178. Tamura, Watanabe, Kato, Yamaguchi, Koike, Komatsu. A delayed phenomena evaluation of prestressed concrete containment vessel at Tsuruga Unit 2 power station. SMIRT 11, 1991.
179. UNSRC Reg. guide 1.35 ISI ungrouted tendons January 1976
180. USNRC Reg. guide 1.90 ISI grouted tendons August 1977
181. Xu Yao Zhang. Containment structure monitoring and prestress losses. Experience from Daya Bay NPP. Joint Wano/OECD-NEA. Workshop, Civaux, Poitiers, France, 1997.
182. Eurocode-3, BSI, 1999, Revision 2002, 2009.
183. Johnson, R.P. and Anderson, D. Designers' Guide to EN 1994-1-1 Eurocode-4. Design of composite steel and concrete structures for buildings. Thomas Telford, 2004.
184. Eurocode-3, Design of Steel Structures. BSI 2004.
185. Shahrooz, B.M. (ed.). Composite Construction in Steel and Concrete. ASCE, New York, 2002, No IV, pp. 584–595.
186. BSI. Design of Concrete Structures.
187. BSI. Design of Structures for Earthquake Resistance, BSI, London, BSEN, 1994.



Structures for Nuclear Facilities

Analysis, Design, and Construction

Bangash, M.Y.H.

2011, XIII, 900 p. 457 illus., 12 illus. in color., Hardcover

ISBN: 978-3-642-12559-1